PNAS

Supporting Information for

Airborne Disease Transmission During Indoor Gatherings Over Multiple Time Scales: Modeling Framework and Policy Implications

Avinash K. Dixit, Baltazar Espinoza, Zirou Qiu, Anil Vullikanti, Madhav V. Marathe

Corresponding Author name.
E-mail: dixitak@princeton.edu, marathe@virginia.edu

This PDF file includes:

Supporting Information Text

Related literature

Infection processes in closed spaces were first examined by Wells. In his pioneering work (1), Wells introduced the concept of *quantum*, defined as "the number of infectious airborne particles required to infect". Later, the work by Riley (2) studied disease transmission in a confined space exploring the impact of different control measures and ventilation rates. In a subsequent work by Riley, Murphy and Riley (3) extended Riley's previous model with Wells' definition of the quanta of infection. The Wells-Riley model incorporates a probabilistic process of infection based on the average quanta of infection inhaled by susceptible individuals. They show an exponential increase in the number of new infections occurs when the quanta-level is assumed at a steady-state during the school day, and in the absence of biological virus decay. In contrast to the aforementioned work, our modeling framework focuses on transmissions between consecutive meetings with potentially varying schedules, such that infected individuals and a certain volume of virus particles could be carried over from one meeting to another. We incorporate the transient dynamics over meetings, the disease dynamics over the population across days, and the efficiency of non-pharmaceutical interventions (NPIs), i.e. mask wearing. In addition, our modeling framework incorporates several parameters grounded in physical conditions of the venue and in individual behavior, that enables us to quantify and compare the effects of several policy measures such as room size, crowd size, mask mandates, reductions in meeting times, lengths of breaks between successive sessions.

Gammaitoni and Nucci (4) studied indoor disease transmission assuming that both, the virus exhalation per infected and, the rate of viral stocks removal by ventilation are constants. Further, the infection risk is assumed homogeneous across the group, and effectiveness of masks are considered in decreasing the infection probability. This model was applied recently to study superspreading indoor events of SARS-CoV-2 (5). While our model incorporates a similar infectious mechanism, the time-scale implicit in the problem we address differs from the Gammaitoni and Nucci paradigm. In particular, we investigate the stationary disease dynamics attained over subsequent meetings for which the viral load can be carried over. In contrast, Gammaitoni and Nucci focus on weekly meetings for which no prior source of quanta in the space is assumed during each meeting.

The role of viral load has been studied from different perspectives and scales. For instance the work by Dodd and Watts (6) consider a group where each susceptible person meets one other person at a time, and from each infected person met, the susceptible host picks up a random viral load. In this work, the authors assumed that if the load exceeds a threshold, the person's likelihood of getting the disease increases sharply. Thus the probability of infection depends on the number of people one meets. Our modeling framework differs in this regard, while in our model the environmental viral load increases as more infected individuals exhale virus in the meeting room, the within host's viral load does not increases by meeting individuals. Instead, we envision the viral load as an intrinsic characteristic of the environment where individuals sojourn.

Jang et al (7) consider infections like MRSA (methicillin-resistant Staphylococcus aureus) or C-diff (Clostridium difficile) that spread via contaminated surfaces, mostly in medical facilities. They model a dialysis unit with movement of healthcare workers from one patient to another and to and from dialysis chairs and nurses' stations that can carry the organisms. In our setting the transmission is airborne, and individuals directly contaminate this air like a "public bad" without any human intermediation.

Hekmati et al. study the spread of airborne disease in enclosed space under individual-level behavioral response (e.g., mask-wearing and vaccination). There are key differences between the work by Hekmati et al. (8), and the proposed model: (i) the scale of Hekmati's work considers a spatially structured population (a school campus), while our proposed model focus on the disease dynamics observed in a particular group

having multiple meetings; (ii) moreover, the time-scale of the disease dynamics in Hekmati's work is slower by considering a unit time of a week, our model aims to address faster disease dynamics with a time unit of a meeting (that can vary in duration with unit time of hours); (iii) for simplicity our model assumes homogeneous individual viral shedding, and homogeneous infection probabilities; finally, (iv) the main difference between our modeling framework and the one by Hekmati et. al., is the formulation of the room-scale airborne virus concentration assumed at the steady state, without assuming virus removal due to settling.

Buonanno et al. (9) derive quanta emission rate of infected individuals under the assumption that droplets and sputum have the same viral load. They then characterized quanta concentration of the disease and transmission risk based on the emission rate. Zafarnejad and Griffin (10) study the spread of COVID-19 in a closed environment (e.g., classrooms). They extend the viral-load model by Buonanno et al. (9), where the transmission risk are now heterogeneous such that it depends both on accumulated viral load and vicinity of infected individuals. Different from both models, our framework incorporates individual behavioral responses and accounts for the effectiveness of mask wearing in discounting viral emission and inhalation.

Loy and Tosin (11) consider a network model where vertices are spacial locations and edges represents connection between locations. Specifically, the disease transmission happens in each location which contains a number of individuals, and the transmission rate depends on the viral load of each individual. Different from their model, the infection rate in our model is a function of the accumulated viral load in a spacial location. Further, we accounts for the efficiency of NPIs such as mask wearing in hindering the spread of disease.

Frazier et al. (12) propose a multi-group simulation framework to study spread of COVID on college campuses. In particular, individuals are divided into different groups, and the disease transmission within and between each group is modeled by a Markov chain. Further, the individual-level disease progression consists of multiple compartments (e.g., Susceptible, Exposed, Quarantine, Isolation). Based on this framework, Frazier et al. study the selection of COVID-19 interventions (e.g., a symptomatic screening program) and model sensitivity to various input parameters. Different from their approach, our model considers epidemic processes within spatial locations, and the disease transmission happens between locations and individuals. Further, we explore the impact of ventilation and class sizes on the disease dynamics.

Bazant and Bush (13) study indoor disease transmission with a focus on sizes of respiratory droplets exhaled by infected individuals. They characterize a critical drop size below which the drops can be sustained in a room for a long time. Based on the findings, they further suggest indoor safety guideline such that one is safer in large rooms with efficient ventilation system. Noakes et al. (14) combined the Well-Riley model with the SEIR model to account for incubation periods for many diseases. They study the impact of model parameters (e.g., the ventilation rate, the occupancy level, incubation period) on disease outbreaks. Issarow (15) There are many other works that study indoor infection from various perspectives (15–18).

Table S1. Model parameters and variables

Parameter	Description	Baseline value
G	Group size	100
A	Air-mass	$9,000$ ft^3
η	Mask efficacy reducing virus exhalation	0.1
α	Mask efficacy reducing virus inhalation	0.3
p	Proportion of the population using face masks	0.5
ρ	Ventilation system efficiency	0.1
δ	Coefficient linking hazard rate to virus load	0.226
ϕ	Recovery rate for infected individuals	0.1
ε	Relative viral shedding of exposed individuals	—
σ	Incubation period	1/9
λ	Rate of loss of immunity for recovered individuals	0.01
τ	Dummy variable of integration over time	
κ	Per-person viral shedding	
ω	Linear approximation of the likelihood of infection	
Λ	Recruitment probability	
v	Flow of virus exhalation by infected individual	
$V(t)$	Virus stock in the space at time t	
$W(T)$	Cumulative virus quantity inhaled over time T	
$P_n(T)$	Infection probability of non-masked susceptible individuals	
$P_m(T)$	Infection probability of masked susceptible individuals	

Table S2. Variations in room parameters

Room size (ft.)	Distancing (ft.)	Group size
20×20	3	25
20×20	6	4
30×30	3	81
30×30	6	16

Table S3. Scenarios, control variables and policy insights.
(a) Group size, (b) air mass (room size), (c) mask compliance, (d) ventilation, (e) break times, (f) testing. We discuss scenarios of meeting periods of 50 minutes (short meetings), and 120 minutes (long meetings). For our simulations we used the baseline parameter values.

Scenario	**Description**	**Control variables**	**Policy insights**
Short time-scale	Single meeting at a single day	a, b, c, d	For short meetings, ventilation and masking have similar effects. For long meetings, ventilation has a greater impact than masking.
Medium short time-scale	Multiple meetings at a single day	a, b, c, d, e	For short meetings, break times of $10-15$ minutes have a similar impact than 50% mask compliance. For long meetings, break times of $20-25$ minutes have a similar impact than 50% mask compliance.
Medium long time-scale	Single meeting at a multiple days	a, b, c, d, f	For short meetings, masking and testing shows a trade-off of 2:1 For long meetings, masking and testing shows a trade-off of 1:1.
Long time scale	multiple meetings at multiple days	a, b, c, d, e, f	For short meetings, a 60% testing reduction is balanced by around 20 minutes breaks. For long meetings, a 40% testing reduction is balanced by around 20 minutes breaks.

Within-meetings dynamics formulation

We let the group size to be determined based on the room size and the targeted physical distancing with the following assumptions; (i) each individual is a point in the plane that takes zero space and, (ii) individuals

are positioned in a grid layout. We consider two potential scenarios for the viral dynamics across meetings: (i) having a single meeting per day and (ii) having multiple meetings per day.

Cumulative viral load and infection probabilities formulation. In this section we show the formulation of the cumulative viral load ($W(t)$) and the infection probabilities ($P_n(t)$,$P_m(t)$) for the scenarios having a single meeting per day. Analogous derivations work for the computation of the cumulative viral load and the infection probabilities for the scenarios having multiple meetings in a single day.

Recall from the main text that the virus exhalation rate is given by $v = k(\eta I^m + I^n)$, where the superscripts denote the masked and unmasked population, respectively. The virus stock V evolves according to $dV/dt = v - \rho V$. Given the initial condition is $V(0) = 0$, and the solution for $V(t)$ is of the form

$$V(t) = \frac{v\,(1 - e^{-\rho t})}{\rho}. \qquad [1]$$

Solving Eqn. (2) in the main text and using equation (SI-1) for $V(t)$, we have

$$\frac{d\ln(1 - P_n(t))}{dt} = -\frac{\delta v}{\rho A}\left(1 - e^{-\rho t}\right), \qquad [2]$$

and integrating we get

$$\ln(1 - P_n(t)) = -\frac{\delta v}{\rho A}\left(t - \frac{1 - e^{-\rho t}}{\rho}\right), \qquad [3]$$

or

$$P_n(t) = 1 - \exp\left[-\frac{\delta v}{\rho A}\left(t - \frac{1 - e^{-\rho t}}{\rho}\right)\right], \qquad [4]$$

where we have used the initial condition $P(0) = 0$ that applies to the S-types. The analogous solution can be obtained for $P_m(t)$, except that δ is replaced by $\alpha\,\delta$, due to masks efficacy. The cumulative virus quantity $W(t)$ available to be inhaled over the meeting period $[0, t]$ is given by

$$\begin{aligned} W(t) &= \int_0^t V(\tau)\,d\tau, \\ &= \frac{v}{\rho}\int_0^t \left(1 - e^{-\rho\tau}\right) d\tau, \\ &= \frac{v}{\rho}\left[t - \frac{1 - e^{-\rho t}}{\rho}\right]. \end{aligned} \qquad [5]$$

Then, the probabilities of infection up to time $t \in [0, T]$, for the masked and unmasked susceptible individuals, can be expressed in terms of the cumulative virus inhalation:

$$P_n(t) = 1 - \exp[-\delta\,W(t)/A], \quad P_m(t) = 1 - \exp[-\alpha\delta\,W(t)/A]. \qquad [6]$$

Moreover, consider the limit scenario of the cumulative amount of virus available to be inhaled over the whole meeting period $[0, T]$, this is given by

$$W(T) = \int_0^T V(\tau)\,d\tau = \frac{v}{\rho}\left[T - \frac{1 - e^{-\rho T}}{\rho}\right] \qquad [7]$$

consequently, the probabilities of infection during the whole meeting for no masked and masked individuals are

$$P_n(T) = 1 - \exp[-\delta\,W(T)/A], \quad P_m(T) = 1 - \exp[-\alpha\delta\,W(T)/A]. \qquad [8]$$

Properties of the cumulative virus stock during the whole meeting, $W(T)$**.** In order to study the impact of the meeting length on the probabilities of infection, we study the properties of the cumulative virus stock $(W(T))$ available for inhalation during the meeting time $[0, T]$:

$$W(T) = \int_0^T V(\tau)\, d\tau = v \left[T - \frac{1 - e^{-\rho T}}{\rho}\right]. \qquad [9]$$

Differentiating equation (SI-9),

$$W'(T) = V(T) = \frac{v\left(1 - e^{-\rho T}\right)}{\rho}, \qquad [10]$$

and

$$W''(T) = V'(T) = v\, e^{-\rho T} > 0. \qquad [11]$$

Therefore, $W(T)$ is an increasing and convex function of t, with $W(0) = 0$, but equation (SI-5) shows that for any given t, it is a linear function of v and therefore of G (remember we are regarding v as proportional to G).

Next, note from equation (SI-10) that $W'(T)$ is an increasing function of v, i.e. $\partial^2 W/\partial v \partial \mathrm{T} > 0$. Therefore, T and v (or equivalently, G) are complements: the marginal increase in $W(T)$ resulting from a marginal increase in the meeting length T, is worse if G is higher. Finally, from equation (SI-1) and equation (SI-5), we have

$$W(T) = v \int_0^T \frac{1 - e^{-\rho\tau}}{\rho}\, d\tau,$$

and for any t,

$$\begin{aligned}\frac{\partial}{\partial \rho}\left[\frac{1 - e^{-\rho t}}{\rho}\right] &= \frac{\rho t e^{-\rho t} - (1 - e^{-\rho t})}{\rho^2}, \\ &= \frac{(1 + \rho t) - e^{\rho t}}{\rho^2\, e^{\rho t}}, \\ &< 0,\end{aligned}$$

therefore

$$\frac{\partial W(T)}{\partial \rho} = v \int_0^T \frac{\partial}{\partial \rho}\left[\frac{1 - e^{-\rho\tau}}{\rho}\right] d\tau < 0.$$

Thus, $W(T)$ is a decreasing function of ρ; consequently higher efficiency of filtration lowers the cumulative virus inhalation during the meeting. This is intuitively obvious, but the exact expression enables us to find the interaction with meeting length:

$$\frac{\partial}{\partial T}\left[\frac{\partial W(T)}{\partial \rho}\right] = v\, \frac{\partial}{\partial \rho}\left[\frac{1 - e^{-\rho t}}{\rho}\right] < 0. \qquad [12]$$

Thus, increasing the meeting time decreases $\partial W(T)/\partial \rho$, i.e. higher filtering efficiency is even more important for longer meetings. Similar calculations for the mask inhalation and exhalation parameters α and η show that improving these efficiencies is even more important for longer meetings.

Properties of the unmasked/masked infection probabilities, $P_n(T)$ ***and*** $P_m(T)$**.** The dependence of $P_n(T)$ on some parameters examined one at a time is quite obvious. For example

$$P_n'(T) = \frac{\delta v}{\rho A}\left(1 - e^{-\rho T}\right)\exp\left[-\frac{\delta v}{\rho A}\left(T - \frac{1 - e^{-\rho T}}{\rho}\right)\right], \quad [13]$$

and

$$\frac{\partial P_n(T)}{\partial v} = \frac{\delta}{\rho A}\left(T - \frac{1 - e^{-\rho T}}{\rho}\right)\exp\left[-\frac{\delta v}{\rho A}\left(T - \frac{1 - e^{-\rho T}}{\rho}\right)\right], \quad [14]$$

are both positive. Remember that v is proportional to G, so the effects of group size can be found by using v as a proxy for it.

The hazard rate (the probability of being infected in a small interval of time $[t, t + dt]$ conditional on not having been infected before time t) is assumed to be a function of the virus concentration in space at time t, and assumed to be linear to allow simple explicit solution, included as Eqn (2) in the main manuscript:

$$\frac{dP_n/dt}{1 - P_n} = \delta\frac{V(t)}{A}. \quad [15]$$

Next consider the curvature of $P_n(T)$. Notice that $P_n(T)$ is an increasing function, where $P_n(0) = 0$ and, from equation (SI-4) we see that $P_n(T) \to 1$ as $T \to \infty$. Therefore the most likely shape of $P_n(T)$ is sigmoidal. To verify this formally, we write equation (SI-15) as

$$P_n'(T) = \frac{\delta}{A}V(T)[1 - P_n(T)], \quad [16]$$

consequently

$$P_n''(T) = \frac{\delta}{A}\left\{V'(T)[1 - P_n(T)] - V(T)P_n'(T)\right\}. \quad [17]$$

Eq. (17) is positive if and only if

$$\frac{V'(T)}{V(T)} > \frac{P_n'(T)}{1 - P_n(T)}. \quad [18]$$

Further, the stock V of the virus in the space at time t evolves according to

$$\frac{dV}{dt} = v - \rho V. \quad [19]$$

Then, using equations SI-19 and SI-15, equation SI-18 becomes

$$\frac{v - \rho V(T)}{V(T)} > \frac{\delta V(T)}{A}, \quad [20]$$

or

$$v > \rho V(T) + \frac{\delta}{A}[V(T)]^2. \quad [21]$$

Since as T goes from 0 to ∞, $V(T)$ increases from 0 to v/ρ, the right hand side of this inequality increases from 0 to $v + (\delta/A)\,(v/\rho)^2$. Thus the inequality is true for small T and false for large T. So $P_n''(T)$ starts out positive and then turns negative, confirming that the shape of $P_n(T)$ is sigmoidal. A similar calculation applies to $P_m(T)$, with the δ on the right hand side of equation (SI-21) changed to $\eta\delta$.

Incidentally, $P_n'(T)$ is maximized (the probability of infection rises fastest, i..e. the incremental harm from lengthening the meeting by another minute is highest) at the inflection point, which occurs when

$v = \rho V(T) + \frac{\delta}{A}[V(T)]^2$ Therefore it may therefore be important to keep the length of the meeting well below this threshold. To find this value, write

$$Y = 1 - e^{-\rho T},$$

so

$$V(T) = v\,Y/\rho,$$

and the equation becomes

$$1 = Y + \frac{\delta\, v}{\rho^2\, A}\, Y^2 = Y + Y^2/b, \quad \text{where} \quad b = \frac{\rho^2\, A}{\delta\, v},$$

or

$$Y^2 + b\,Y - b = 0,$$

where the feasible solution is

$$Y = \left[-b + (b^2 + 4\,b)^{1/2}\right]/2,$$

keeping the positive root to get $Y > 0$. Then

$$T = -\frac{\ln(1-Y)}{\rho}. \qquad [22]$$

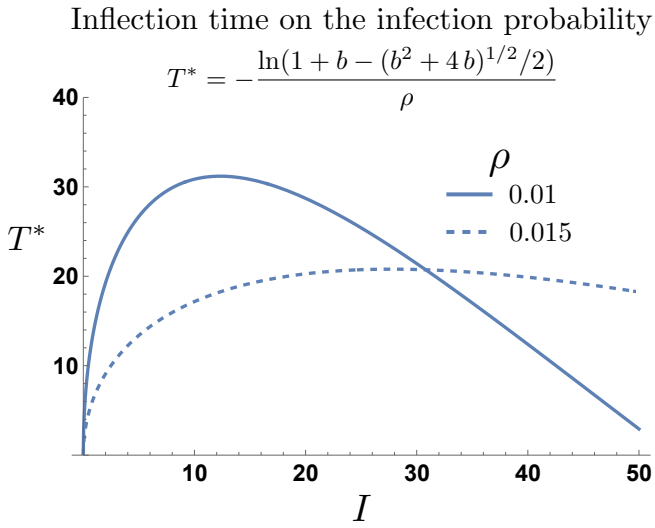

Fig. S1. Inflection time T of the probability of infection as a function of the number of infected individuals I.

Now consider $P_n(T)$ for a given T as a function of v. We see from equation (SI-4) that it is a concave function, starting at zero when $v = 0$, and rising to 1 as $v \to \infty$. (alternatively, we can see from equation (SI-14) that $\partial P_n(T)/\partial v$ is a positive and decreasing function of v.) Therefore it is not clear whether longer time or larger crowd size are more risky. If T is in the region to the left of the inflection point of $P_n(T)$ (i.e. where $P_n''(T) > 0$), then the comparison is as it was for the cumulative virus inhalation $Q(T)$, i.e. splitting a long meeting into two halves is better than splitting the crowd into two, each of the halves taking the full meeting in one session. But if the duration is beyond the point of inflection, the comparison could go either way.

Next consider the interaction between T and v (the latter is in turn proportional to G). For brevity of notation, write equation (SI-13) as

$$P_n'(T) = hve^{-kv}, \quad [23]$$

where

$$h = \frac{\delta}{\rho A}\left(1 - e^{-\rho T}\right) \text{ and } k = \frac{\delta}{\rho A}\left(T - \frac{1 - e^{-\rho T}}{\rho}\right) \quad [24]$$

are both positive and depend on T but not v. Then

$$\frac{\partial^2 P_n}{\partial v \partial T} = he^{-kv} - hkve^{-kv} = he^{-kv}(1 - kv). \quad [25]$$

Using the full expression for k, this cross-derivative is positive (T and G are complements) if $kv < 1$, that is

$$\frac{\delta v}{\rho A}\left(T - \frac{1 - e^{-\rho T}}{\rho}\right) < 1. \quad [26]$$

This is true if G and T are both small, and false if one or both are large. So if we conduct a thought-experiment of starting with a small crowd that gathers for a short time, and increase these magnitudes gradually, initially increasing one increases the marginal risk posed by the other, but eventually the effect goes the other way. This again contrasts with the clear result (complements) we found for $Q(T)$.

The calculation for S-types wearing a mask is similar, except δ is reduced by a factor α to $\alpha\delta$, where $0 < \alpha < 1$ captures the efficiency of masks in reducing virus inhalation; lower α implies higher efficiency. At the extremes, if $\nu \cong 0$ or A is large (open air), then $P(t) \cong 0$ for all t; if both v and T are positive and one of them is large, then $P(T) \cong 1$. (Note that in the latter case even the masked are almost sure to get infected.)

Upper bound on probability of infection. Let $T \geq 0$ be the length of a single meeting. Suppose the objective is to keep the probability below some desired threshold. For this, we have to keep $W(T)/A$ below an appropriate threshold. This criterion depends on T and the other parameters, so examining this dependence tells us how various changes make it easier or harder to meet such a target.

One can verify that $W(T)$ is an increasing and convex function of T, with $W(0) = 0$. Moreover, for any given T, $W(T)$ is a linear function of v and therefore of G (recall that v is proportional to G). This yields a trade-off between increasing the length of meeting time and increasing the number of participants. For example, if one has to give a 2-hour lecture to 100 people, they get less cumulative virus inhalation if the lecture is split into two 1-hour segments with the full audience (with a complete air change in the auditorium between the halves so the second half also starts with $V(0) = 0$), than if the audience is split into two groups of 50 and subjected to the full 2-hour lecture given separately for each ($2\,W(T/2) < W(T)$, and $2\,W(G/2) = W(G)$).

Next, $W'(T)$ is positive and an increasing function of v. Therefore T and v (or equivalently, T and G) are complements: the increase in $W(T)$ resulting from a marginal increase in T is bigger if G is higher. Thus longer meetings are all the worse for keeping the probability of infection below the desired threshold if the group size is larger. Finally, a greater filtration efficiency ρ reduces $W(T)$, and this negative effect becomes even larger in magnitude when T is larger. Therefore a higher filtering efficiency is even more important for long meetings. Similar calculations for the mask inhalation and exhalation parameters α and η show that improving these efficiencies is even more important for longer meetings.

These above results apply to the cumulative virus inhalation $W(T)$. The probability of getting the disease – $P_n(T)$ or $P_m(T)$ depending on the masking type – is a nonlinear function of $W(T)$. Therefore, if the

objective is not simply keeping the disease probability below a specified level, but a more general function involving some expected cost, so the magnitude, not just the direction, of the effect on the probabilities matters, we have to look at the effects of various parameters on $P_n(T)$ and $P_m(T)$ directly. This is done next.

Magnitudes of the probability of getting the disease. The shape of $P_n(T)$ and $P_m(T)$ as functions of T is sigmoidal: each starts out at $T = 0$ with zero slope, then rises as a convex function, becomes concave at an inflection point t^*, and then asymptotes to a unit. The inflection point is where the infection probability rises fastest. Therefore it is useful to know this point for plausible values of the various parameters, to reduce the meeting times below it to get the sharpest reductions in infection probabilities.

Next consider the interaction between the meeting time T and the group size G (or equivalently v), in affecting the probabilities $P_n(T)$ and $P_m(T)$. We see from (4) that $P_n(T)$ is an increasing concave function of v, and to the left of the inflection point it is an increasing convex function of T. Therefore in this region the comparison is as it was for the cumulative virus inhalation $W(T)$, i.e. splitting a long meeting into two halves is better than splitting the crowd into two, each of the halves taking the full meeting in one session. But if the duration is beyond the point of inflection, the comparison could go either way.

Are the two complements, i.e. is $\partial^2 P_n/\partial v \partial T$ positive? We find that to be the case, if G and T are both small, and false if one or both are large. So if we conduct a thought-experiment of starting with a small crowd that gathers for a short time, and increase these magnitudes gradually, initially increasing one increases the marginal risk posed by the other, but eventually the effect goes the other way. This again contrasts with the clear result (complements) we found for $Q(T)$. Again, a similar analysis applies to $P_m(T)$.

Our results fit well within the range of typical meeting times for lectures or theater performances or dinners. Reducing these times by even a little would pay big dividends in reduced probabilities of infection. For example, consider a 60-minute lecture with an audience of 100. If one infected student gets in, the probability that one of the rest is exposed by the end of the lecture is 1.248%. However, if the lecture were only 50 minutes long, this would be reduced to 1.001%. Which translates in a a significant reduction of the basic reproductive number $\mathcal{R}_0$.

Modeling multiple time-scale scenarios

In this section we explore the multiple scenarios that our model formulation can address, the difference between them is the variation of the time-scales involved. The scenarios we consider address potential meeting scenarios occurring at different time-scales. We consider two short time-scale scenarios and two long time-scale scenarios. In the short time-scale scenarios, individuals gather for a single or multiple meetings during a single day. At this time-scale there are no dynamics at the population's scale. We track the dynamics of the viral load in the meeting room and, ultimately the expected number of newly exposed individuals. In the long time-scale scenarios, individuals gather for a single or multiple meetings, during multiple days. At this time-scale we track the "fast dynamics" of the viral load and, the "slow dynamics" of the disease spreading in the population. We assume the contagion process starts with a single unmasked infected individual attending the first meeting.

Short time-scale: Single meeting on a single day. In this scenario, we capture the dynamics of events happening in a single meeting at a single day, for instance people attending a bar or a party. We assume individuals meet at a single day for a determined period of time and, we focus on the number of secondary cases generate during the meeting. We let, the number of infected individuals attending the meeting to be constant. Moreover, due to the short time-scale involved, we do not address population-level dynamics.

In order to compute the number of secondary cases generated during the meeting, we incorporate the room conditions stated in our model. The probabilities of getting exposed during the meeting depend on the number of masked/unmasked infected individuals present in the meeting and, are given by the viral load attained during the meeting, and described by Eqns. (3) and (5) of the main text. We let the number of susceptible/infected individuals, as well as the masked/unmasked individuals to be given as initial conditions, and we track the number of exposed individuals for different group sizes and mask wearing compliance. Since newly exposed individuals take several days in order to become infectious, we assume the number of individuals shedding virus is constant. In this scenario, the potential interventions include, the ventilation system efficiency (ρ), the room size or equivalently the group size or population density (G), mask wearing and compliance (d).

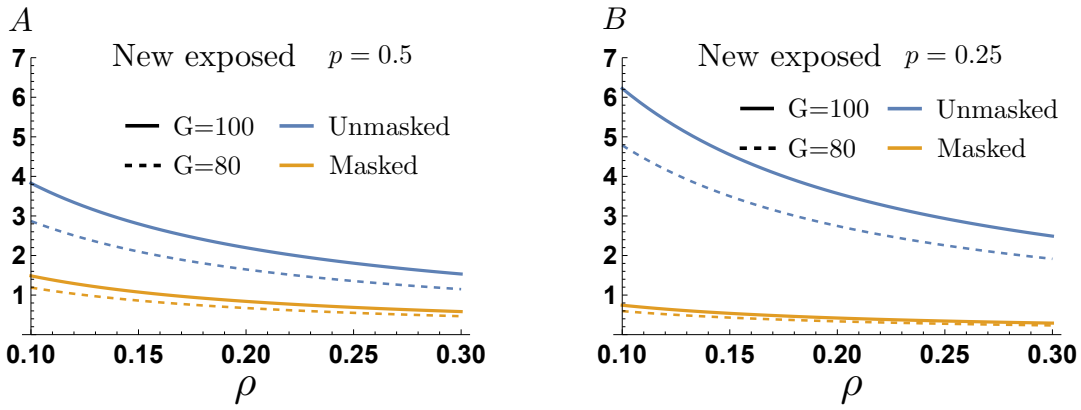

Fig. S2. The impact of improving ventilation system efficiency (ρ), for group sizes $G = 100$ and $G = 80$, when 50% and 25% of the participants use masks, for a meeting length of $T = 50$ minutes. For our selected simulations we assume $I_n = 10$ and $I_m = 0$.

Figure S2 show the number of newly masked and unmasked exposed individuals after a single meeting, as a function of the ventilation system efficiency (ρ), for the scenarios of group sizes $G = 100$ and $G = 80$, assuming a 50% and a 25% of the attendants use face masks. Intuitively, increasing the ventilation system efficiency plays a bigger role as less attendants wear face masks.

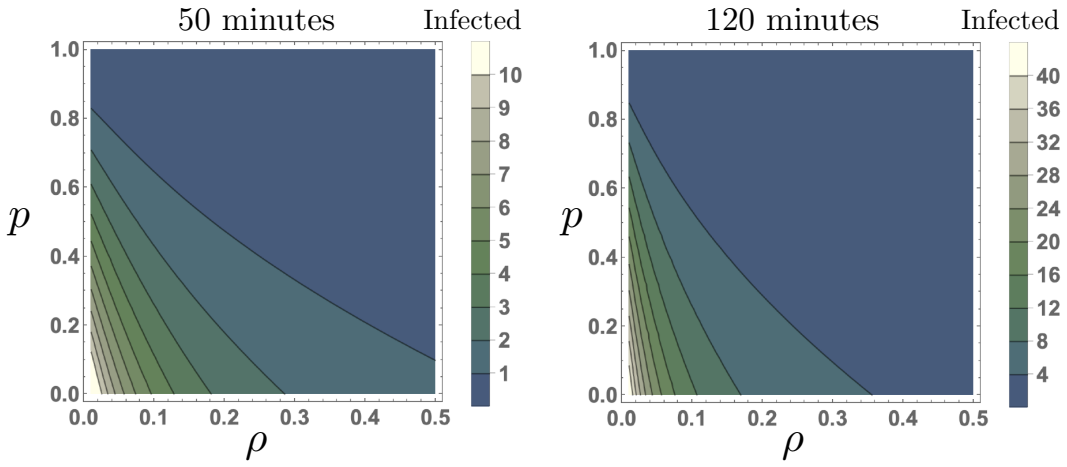

Fig. S3. Trade-off between the ventilation system efficiency (ρ) and mask compliance (d).

Figure S3 shows that during short meetings the impact of increasing the ventilation system efficiency is comparable to the impact of increasing mask compliance. However, during long meetings, the overall impact of having a better ventilation system overcomes the impact of increasing mask compliance. This is

an intuitive result since our model formulation shows that even with high mask compliance, the role of the ventilation system efficiency is critical on maintaining the viral load at low levels, see Eq. (12).

Medium short time-scale: Multiple meetings on a single day. This scenario resembles the meeting dynamics of single day events hosting multiple meetings with breaks between one meeting to another, for instance at a conference or a single day at school. We focus on the number of expected secondary cases generated after each meeting. At this medium short time-scale, we let the number of susceptible/infected individuals, as well as the masked/unmasked individuals to be given as initial conditions. Similar to the single meeting scenario, we assume the number of individuals shedding virus is constant.

In this scenario, in addition to the previously discussed potential interventions, managing the break time between meetings to let the viral load decrease due to the ventilation system represents another potential intervention.

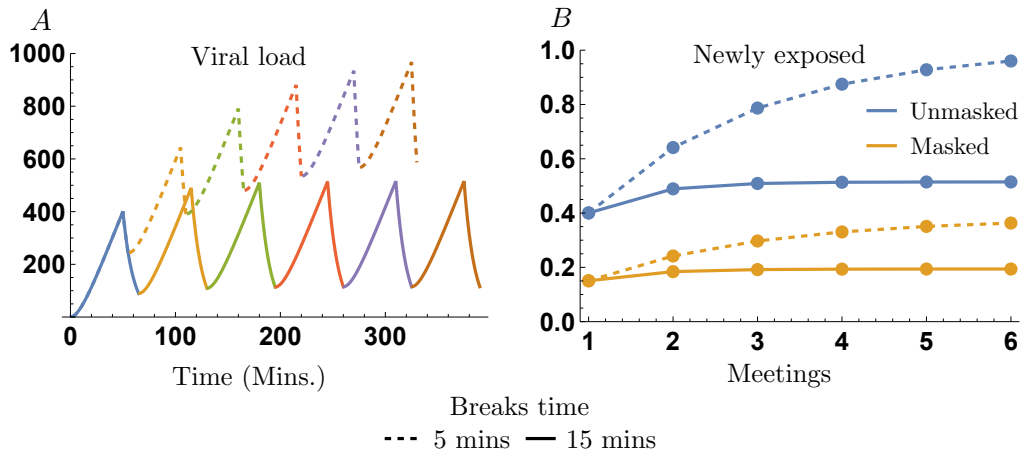

Fig. S4. Viral load for multiple meetings in a single day, for inter meetings break times of 5 and 15 mins. For our selected simulations we assumed $G = 100$, $I_n = 10$, $I_m = 0$, and $d = 0.5$.

Our simulations in Figure S4A show that for break times of 5 minutes, the highest cumulative viral load (attained at the end of each meeting) follows an increasing trajectory during the first six meetings. In counterpart, for break times of 15 minutes, the highest cumulative viral load reaches an steady state after the second meeting. The divergence in the viral load trajectories is ultimately reflected in the number of secondary cases generated over the meetings series. Figure S4B shows that break times of 5 minutes would continue to generate secondary cases after the sixth meeting. The unmasked population is expected to generate more than a single newly exposed individual after the sixth meeting. On the other hand, the bounded viral load attained for meetings with 15 minutes breaks, makes the expectation of the newly exposed individuals to stay below 1.

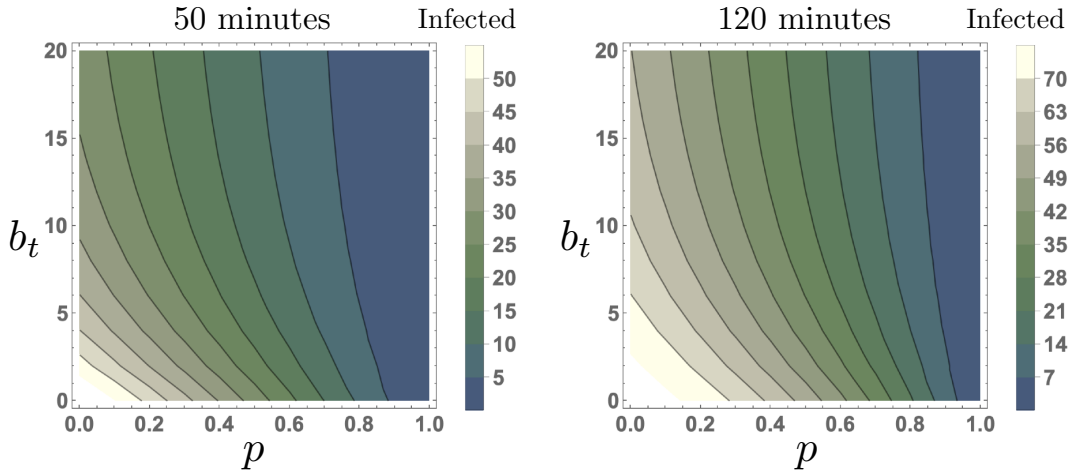

Fig. S5. Trade-off between the break time (b_t), and mask compliance (d), on the number of secondary cases produced in 6 subsequent meetings in a single day.

Figure S5 shows that, in the subsequent meetings schedule, break times are effective interventions to avoid reaching high viral load levels and therefore high infection probabilities. For instance, break times of $15 - 20$ minutes, after each meeting of 50 minutes, lead to similar infection levels than a meetings schedule with no breaks with mask compliance of 50%. Moreover, for schedules where the meeting period is extended to 120 minutes, break times of 20 minutes are required in order to attain the infection levels corresponding to 50% of mask compliance.

Medium long time-scale: Single meetings on multiple days. In this scenario, we assume individuals meet once per day, during multiple days. This scenario was also discussed in the main manuscript.

Extreme scenarios: All uses masks versus no one uses masks. Figures S6 and S7 show the graphs of the two cases; assuming the time-scale scenario of hosting a single meeting per day, during multiple days. By assuming the epidemic starts with a single unmaked infected individual, we simulate 200 meetings, by which time the dynamics in both cases have reached an stationary state with initial small oscillations.

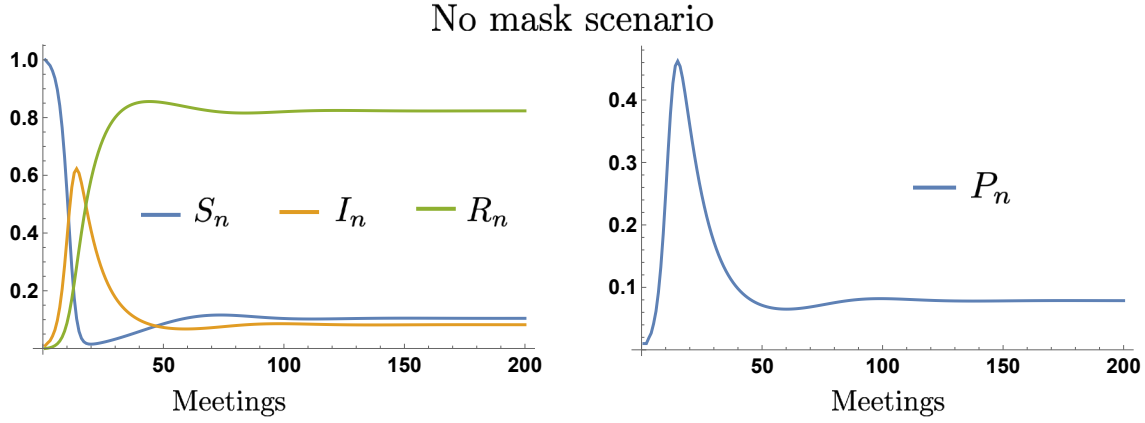

Fig. S6. Dynamics of the unmasked population (S_n, I_n, R_n) and their infection probability (P_n) over iterative meetings.

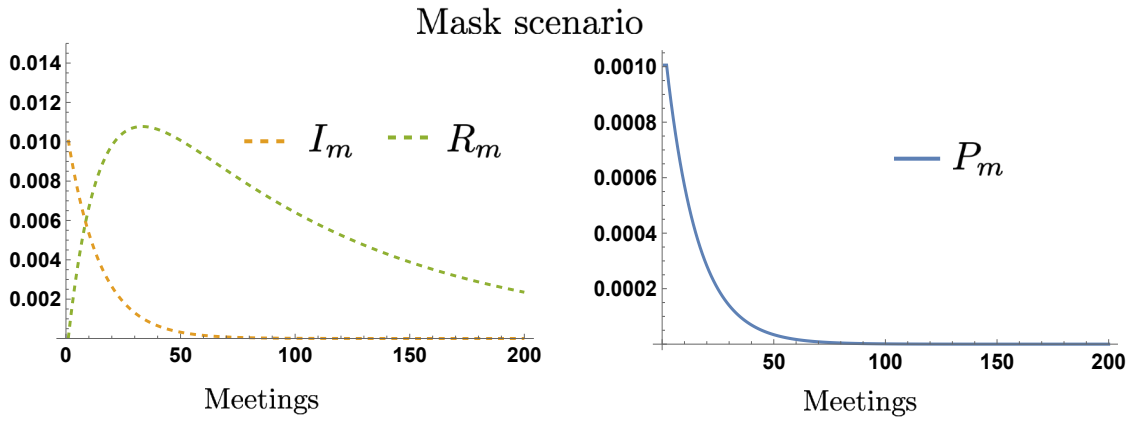

Fig. S7. Dynamics of the masked population (S_m, I_m, R_m) and their infection probability (P_m) over iterative meetings.

The most striking feature of these cases is the dramatic difference made by mask-wearing. Without masks, and assuming a single index individual the disease propagates into an epidemic that at its peak (by meeting 10) has over two-thirds of the population infected and another quarter who have been previously infected and have now recovered. At the first meeting, the index case creates a 1% probability of infecting the 99 others susceptible. Which is in expectation almost one new infection.

This for the small probability that the index case will have recovered before entering the second meeting, that meeting will have in expectation 1.89 infected people, generating a probability 1.88% of infecting a susceptible at the second meeting, resulting in almost 2 new infections from the 98 susceptibles. This almost geometric growth continues, until sufficiently few susceptibles are left, and sufficiently many of the infected have recovered with immunity, to dampen the spread. However, around meeting 15 even though there are almost no susceptibles, there are over 50% infected, and almost 50% recovered, so they had been infected in the past. That is, almost the whole population has experienced the disease. Moreover, as the recovered start to lose their immunity, they become susceptible again, and the epidemic continues, albeit with somewhat less force.

The scenario where everyone wears masks is quite different. The index case in meeting 1 has only a 0.03% probability of infecting someone else. We see the reason from the expression for $P_m(T)$ and $P_n(T)$. The argument for the exponential on the right hand side of $P_m(T)$ has a factor α, and since we are considering here a scenario where everyone wears a mask ($I_n = 0$), it also has a factor η coming from the v. In equation (SI-4), since no one wears a mask, $P_n(T)$ lacks both these factors; and, for small positive x, $1 - \exp(-x) \approx x$. Therefore $P_m(T) \approx \alpha\,\eta\,P_n(T)$: the risk of infection is reduced by the efficiency factors of both the infected exhaler and the susceptible inhaler of the virus. Then the infected seed is almost harmless; in fact the small (in expectation) entry into the second meeting, of a person newly infected by the index case, is more than offset by the less-small probability of recovery of the index case. Therefore, in expectation, the meeting 2 has only 0.93 infected instead of the index case at the first meeting. This continues, and the infection dies down. In fact, experiments using the same parameters show that even with 50% of the population infected at the first meeting, the number of infected dies down around the meeting 33.

In general, although we have not included differential susceptibility in our framework, the parameters ϕ and λ could be different for the masked/unmasked people, some individuals may get more severe disease that has slower recovery and shorter (or perhaps longer) immunity.

Steady state when all or none wear masks. We focus on the extreme cases where all or none of the participants wear masks, we omit the subscripts m and n for convenience. In the no-mask case, we have $v = k\,I$, and the expression for probability of infection in one meeting is $P(T) = 1 - \exp(-\omega I)$, where for

simplicity we define $\omega = \frac{\delta k}{\rho A}\left(T - \frac{1-e^{-\rho T}}{\rho}\right)$.

$$\begin{aligned} S_{j+1} &= (1 - P(T))S_j + \lambda_P(G - S_j - I_j) \\ I_{j+1} &= P(T)S_j + (1 - \phi_P)I_j. \end{aligned} \qquad [27]$$

A similar equation will hold in the all-masked case except that its ω will have additional factors η and α. The steady state for the scenario when no one uses mask in Eq. (27) involves transcendental functions and cannot be analytically computed. Therefore we use a linear approximation of the probability of infection in order to get analytic insights $P(T) = 1 - \exp(-\omega I) = \omega I$. The disease dynamics over the sequence of meetings is then described by the following set of difference equations

$$\begin{aligned} S_{j+1} &= (1 - \omega I)S_j + \lambda_P(G - S_j - I_j) \\ I_{j+1} &= \omega I S_j + (1 - \phi_P)I_j. \end{aligned} \qquad [28]$$

with steady states $(S^*, I^*) = (G, 0)$ and $(S^*, I^*) = \left(\frac{\phi}{\omega}, \frac{\lambda}{\lambda+\phi}(G - \frac{\phi}{\omega})\right)$. In order to compute the disease persistence threshold we use the second generation matrix (19), where $\mathcal{R}_0 = G\frac{\omega}{\phi}$. In other words, the disease persists whenever $\mathcal{R}_0 \geq 1$, which defines a condition in terms of $\omega^* \geq \frac{\phi}{G}$.

Figure S8 shows the phase planes of Eq. (28) parameterized to low recovery/removal probability (A) which leads to a steady state with high disease levels and; middle (B) and high recovery/removal probabilities (C), which lead to intermediate and low disease levels at the steady state, respectively.

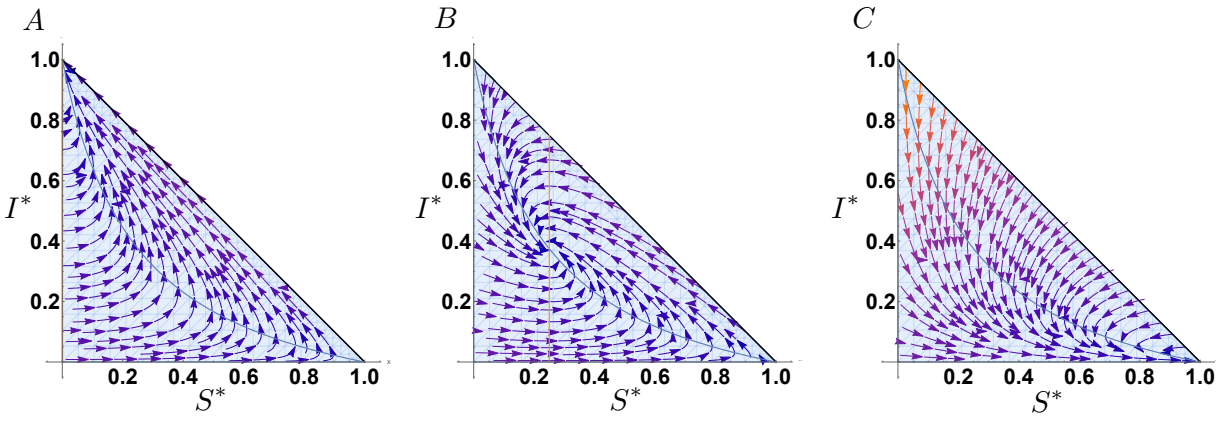

Fig. S8. Existence and stability of the interior equilibrium. Our simulations show that the steady state in the presence of disease may reach states of high, medium and low infectiousness among the population depending on the recovery probability ϕ_P.

The scenario in Eq. (28) corresponds to nobody using masks. Analogous analysis for the scenario where everybody uses masks gives the steady states $(S_m^*, I_m^*) = (G, 0)$ and $(S_m^*, I_m^*) = \left(\frac{\phi}{\alpha\eta\omega}, \frac{\lambda}{\lambda+\phi}(G - \frac{\phi}{\alpha\eta\omega})\right)$. In the scenario where everybody uses masks, the steady state supporting infections exists whenever $\alpha\eta G\omega > \phi$, therefore the threshold condition using masks as a control measure can be expressed as $\mathcal{R}_C(\alpha, \eta) = G\alpha\eta\frac{\omega}{\phi}$. That is, the critical infectiousness is given by $\mathcal{R}_C(\alpha, \eta) \geq 1$ which implies $\omega^*(\alpha, \eta) \geq \frac{\phi}{\alpha\eta G}$.

In agreement with our previous simulations, we show that there exists a set of conditions for which scenarios supporting infections are possible. In Figure S9, we show the bifurcation diagram corresponding to the extreme scenarios where no one uses face mask and, where everybody uses face mask.

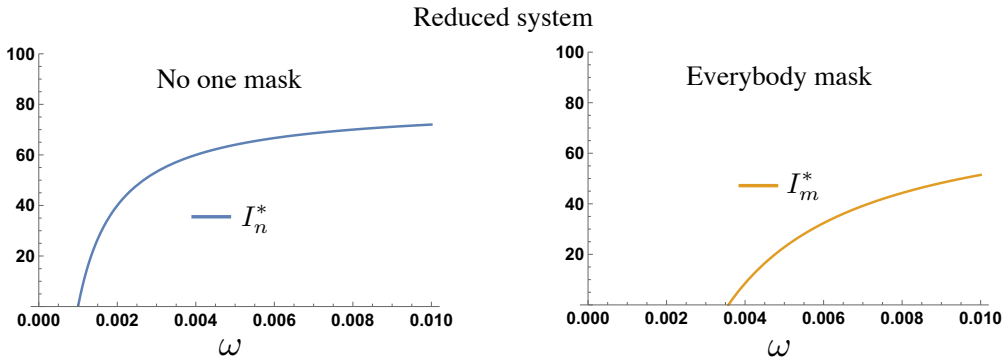

Fig. S9. Bifurcation diagram of the steady states for the extreme scenarios when no one uses face masks (I^*), and when everybody uses face masks (I_m^*), as functions of the parameter ω. Low ω values does not support infected individuals at the steady states, while $\omega \geq \omega^*$ values support the presence of infected individuals in both scenarios. Higher ω value is required for an epidemic to propagate in the extreme scenario of everybody wearing face masks.

Figure S9 shows the double impact of face masks usage: the level of infections attained at the steady state for similar infectious probabilities (ω) is lower when everybody mask, relative to the analogous no masks scenario; and, the infection probability required to sustain infections at the steady state is higher than the one in the absence of masks ($\omega^* \leq \omega^*(\alpha, \eta)$).

Stability of the extreme scenarios steady states: only mask users and, no one uses masks The Jacobian of system Eq. (28) evaluated at the non-trivial steady state is

$$\begin{pmatrix} -\frac{\lambda(\lambda+G\omega)}{\lambda+\phi} & -(\lambda+\phi) \\ \frac{\lambda(G\omega-\phi)}{\lambda+\phi} & 0 \end{pmatrix} \qquad [29]$$

with characteristic polynomial

$$z^2 + \frac{\lambda(\lambda+G\omega)}{\lambda+\phi} z + \lambda(G\omega - \phi). \qquad [30]$$

The sum of the roots is negative, and the product of the roots is positive when $G\omega^* > \phi$ which is the condition for an endemic state with disease ($I > 0$). Then the roots cannot be real and both positive, or real with opposite signs – they must be either real and both negative, or complex conjugates with negative real parts. In either of these possibilities, the steady state is stable. With our basic parameter values, the complex conjugate case (cyclic stability) prevails. Therefore, the steady state $(S^*, I^*) = (\frac{\phi}{G\omega}, \frac{\lambda}{\lambda+\phi}(G - \frac{\phi}{\omega}))$ is stable whenever it exists.

General model: mixed group scenario. In the general model, we let $v = k\,(\eta\, I_m + I_n)$ and the infection probabilities linear approximations become $P_n(T) = \omega\,(\eta\, I_m + I_n)$ and $P_m(T) = \omega\,\alpha\,(\eta\, I_m + I_n)$.

$$\begin{aligned} S^n_{j+1} &= (1 - \omega(\eta I^m_j + I^n_j))S^n_j + \lambda_P((1-p)G - S^n_j - I^n_j) \\ I^n_{j+1} &= \omega(\eta I^m_j + I^n_j)S^n_j + (1-\phi_P)I^n_j. \\ S^m_{j+1} &= (1 - \alpha\omega(\eta I^m_j + I^n_j))S^m_j + \lambda_P(pG - S^m_j - I^m_j) \\ I^m_{j+1} &= \alpha\omega(\eta I^m_j + I^n_j)S^m_j + (1-\phi_P)I^m_j. \end{aligned} \qquad [31]$$

The general model in Eq. (31) has the set of disease-free equilibria $(S^n, I^n, S^m, I^m) = ((1-p)G, 0, pG, 0)$, which depend on the proportion of the group using masks (p), and the following two steady states supporting

non-trivial infection levels

$$
\begin{aligned}
S_n^* &= \frac{(1-\alpha)\phi - \alpha\omega((1-p)G + \eta pG) + \sqrt{x}}{2\omega(1-\alpha)}, \\
I_n^* &= \frac{\lambda\left(-\phi(1-\alpha) - \alpha\omega((1-p)G - \eta pG) + 2(1-p)G\omega - \sqrt{x}\right)}{2\omega(1-\alpha)(\lambda+\phi)}, \\
S_m^* &= \frac{(1-\alpha)\phi + \alpha\omega((1-p)G + \eta pG) - \sqrt{x}}{2\alpha\eta\omega(1-\alpha)}, \\
I_m^* &= \frac{\lambda\left(-\phi(1-\alpha) - \alpha\omega((1-p)G - \eta pG) + 2pG\alpha^2\eta\omega + \sqrt{x}\right)}{2\alpha\eta\omega(1-\alpha)(\lambda+\phi)},
\end{aligned}
\qquad [32]
$$

where $x = (1-\alpha)^2\phi^2 + \alpha^2\omega^2((1-p)G + \eta pG)^2 - 2(1-\alpha)\alpha\omega\phi((1-p)G - \eta pG)$.

Finally, the threshold condition for the full model can be obtained by solving $I_n^* = I_m^*$ from Eq. (32). Thus, the condition for a mixed steady state supporting infection (with or without face masks), is given by

$$
\mathcal{R}_C(d, \alpha, \eta) = \frac{\omega}{\phi}(\alpha\eta pG + (1-p)G) \geq 1 \qquad [33]
$$

which in terms of the probability of infection is $\omega^*(d, \alpha, \eta) \geq \frac{\phi}{\alpha\eta pG + (1-p)G}$. Due to the complexity of the endemic equilibria expressions, we explored their stability numerically. Notice that Eq. (33) reduces to the threshold conditions for the scenarios where all or none uses masks, as a function of d. Figure S10 shows that, similarly to the reduced systems, the full model exhibit a classic forward bifurcation for the infected subpopulations wearing and not wearing masks, as the infectiousness potential (ω) increases. Our simulations show the impact of the mask efficacy on reducing the virus inhalation (α) and virus exhalation (η), by increasing the threshold condition for the infectiousness potential (ω) needed to produce and endemic state.

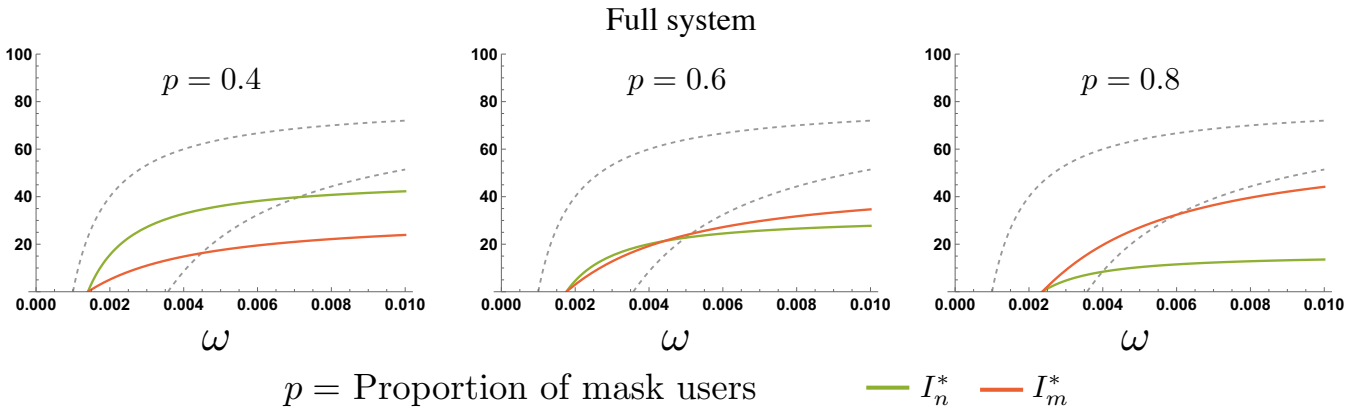

Fig. S10. Bifurcation diagram of the endemic equilibria for the infectious subpopulations (I_n^*, I_m^*), as functions of the parameter ω. The gray dashed lines correspond to the bifurcation trajectories for the reduced scenarios where no one and where everybody uses face masks.

Long time-scale: Multiple meetings on multiple days. In this extreme scenario, we assume individuals meet multiple times per day, during multiple days, for instance students attending school (where in the class composition is fixed), or nursing homes. In this scenario, we track dynamics within consequent meetings (short time-scale dynamics) in a single day, and we compute the number of newly infected individuals. Moreover, we track the dynamics of disease progression over multiple days (long time-scale dynamics), so that the number of infected individuals shedding virus during the daily meetings vary over time.

We compute the meeting-i probability of infection by using the cumulative viral load ($W(t)$), at the end of each meeting. In order to couple short time-scale dynamics we compute the overall probability of

infection during a single day, which is given by the cumulative probability of infection during each meeting. Let the meeting-i probability of infection be p_i, therefore the probability of infection during the day t (after n meetings), is given by

$$P_t = p_1 + p_2(1-p_1) + \cdots + p_n \prod_{k=1}^{k=n-1}(1-p_k) = 1 - \prod_{k=1}^{k=n}(1-p_k). \qquad [34]$$

Figure S11 and figure S12 show the interaction between the inter-meetings viral load (short time-scale dynamics), and the population-level disease dynamics (long time-scale dynamics). We assume a scenario resembling school attendance, that is 6 daily 50 minutes meetings during 7 days, for scenarios of 5 and 15 minutes breaks between meetings. Figure S11A shows a viral load dramatically increasing over meetings, consequently increasing the probability of infection, which ultimately impacts on the number of newly infected individuals. This in turn, results in more infected individuals shedding virus on the room during the subsequent days. The increasing tendency on this feedback loop continues until the population dynamics attain a maximum number of infected individuals, so that the viral shedding over meetings "follows" the population level disease dynamics.

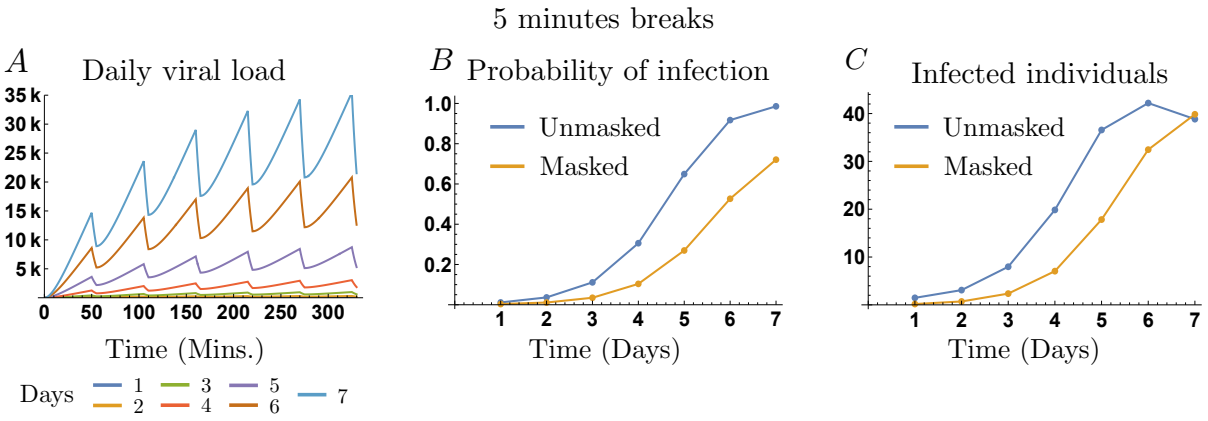

Fig. S11. Viral load, daily probability and infected individuals dynamics, for the scenario of 5 minutes breaks between meetings

In counterpart, the feedback loop shown in Figure S12 exhibit different dynamics across scales. In this scenario, the 15 minutes breaks are long enough to allow the ventilation system clean the environment better. Thus, preventing the daily probability of infection to increase dramatically and, finally ameliorating the impact of the epidemic at the population scale.

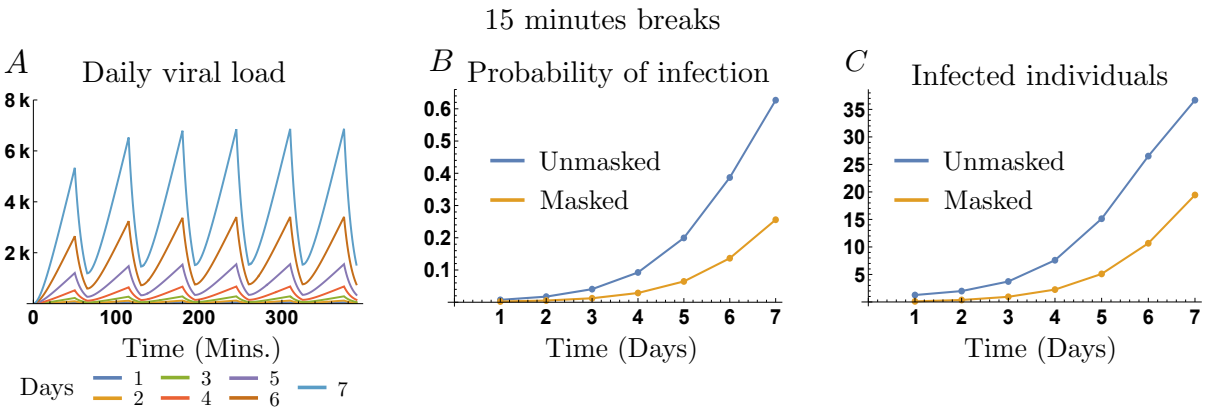

Fig. S12. Viral load, daily probability and infected individuals dynamics, for the scenario of 5 minutes breaks between meetings

Modeling testing

In this section we consider an extension of the baseline model in the main manuscript to include testing. We assume infected individuals are tested and isolated after being identified (Q), until the infected individuals recover. The model incorporating testing becomes

$$\begin{aligned} S^n_{j+1} &= (1 - P^n_j(T))\ S^n_j + \lambda_P\ R^n_j \\ I^n_{j+1} &= P^n_j(T)\ S^n_j + (1-\phi_P)(1-P_{test})\ I^n_j \\ R^n_{j+1} &= (1-\lambda_P)\ R^n_j + \phi_P\ (I^n_j + Q^n_j) \\ Q^n_{j+1} &= (1-\phi_P)P_{test} I^n_j + (1-\phi_P) Q^n_j \end{aligned}$$

$$\begin{aligned} S^m_{j+1} &= (1 - P^m_j(T))\ S^m_j + \lambda_P\ R^m_j \\ I^m_{j+1} &= P^m_j(T)\ S^m_j + (1-\phi_P)(1-P_{test})\ I^m_j \\ R^m_{j+1} &= (1-\lambda_P)\ R^m_j + \phi_P\ (I^m_j + Q^m_j) \\ Q^m_{j+1} &= (1-\phi_P)P_{test} I^m_j + (1-\phi_P) Q^m_j \end{aligned} \qquad [35]$$

Notice that, in the absence of testing ($P_{test} = 0$) model Eq. (36) reduces to the baseline model (7) in the main manuscript.

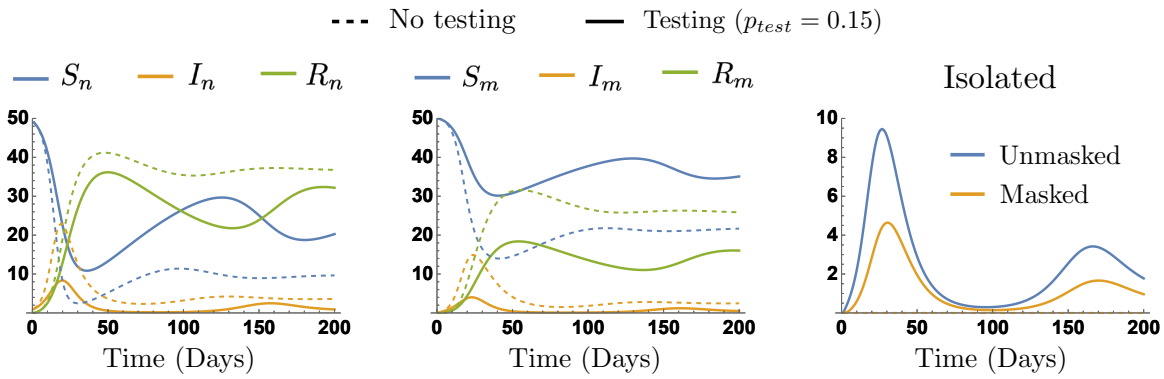

Fig. S13. Disease dynamics of group meetings assuming a single meeting during multiple days, for the scenario of no testing and testing probability $P_{test} = 0.15$.

The impact of including a testing strategy is shown in the dynamics of the viral load attained over meetings, by reducing the number of infected individuals shedding virus.

Steady state when all or none wear masks. In these extreme scenarios, and using a linear approximation for the probability of infection, the model Eq. (36) becomes

$$\begin{aligned} S_{j+1} &= (1 - \omega I_j)\ S_j + \lambda_P\ R_j \\ I_{j+1} &= \omega I_j\ S_j + (1-\phi_P)(1-P_{test})\ I_j \\ R_{j+1} &= (1-\lambda_P)\ R_j + \phi_P\ (I_j + Q_j) \\ Q_{j+1} &= (1-\phi_P)P_{test} I_j + (1-\phi_P) Q_j \end{aligned} \qquad [36]$$

The non-trivial steady state of this model is given by

$$\{S^*, I^*, R^*, Q^*\} = \left\{\frac{\varphi}{\omega}, \frac{\lambda}{\lambda+\phi}\left(\frac{\phi}{\varphi}\right)\left(G - \frac{\varphi}{\omega}\right), \frac{\phi}{\lambda+\phi}\left(G - \frac{\varphi}{\omega}\right), \frac{\lambda}{\lambda+\phi}\left(\frac{(1-\phi)p_{test}}{\varphi}\right)\left(G - \frac{\varphi}{\omega}\right)\right\}. \qquad [37]$$

where $\varphi = \phi + p_{test}(1-\phi)$. Notice that, the non-trivial steady state is meaningful whenever $G - \varphi/\omega > 0$, that is the threshold condition for an epidemic to propagate is given by $\mathcal{R}_0(p_{test}) = G\frac{\omega}{1-(1-p_{test})(1-\phi)}$. Which in the absence of testing $p_{test} = 0$, it reduces to the threshold condition of our baseline SIR model $\mathcal{R}_0 = G\frac{\omega}{\phi}$.

Here we show simulations for the scenario of hosting a single meeting during multiple days, where the model formulation includes the role of testing.

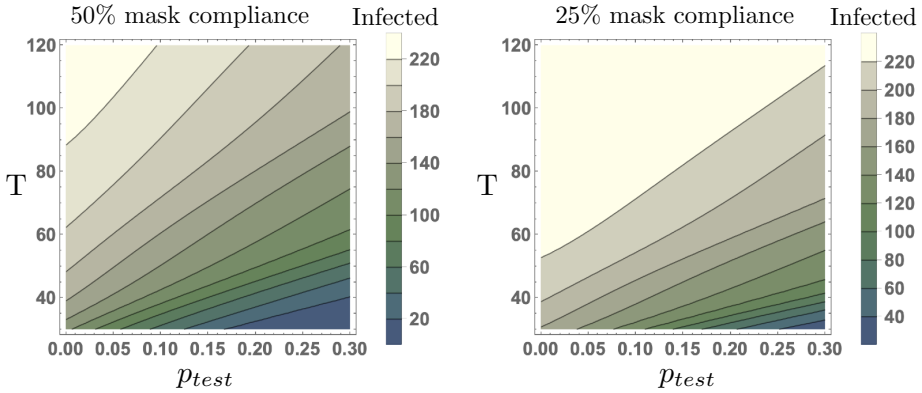

Fig. S14. Trade-off between testing (p_{test}), and meeting length (T), on the cumulative number of secondary cases produced in 60 days having a single meeting, for the scenarios of 50% and 25% mask compliance.

Figure S14 suggest that, for meetings longer than 30 minutes, for each increment on the meeting time of around 10 minutes, it would require to increase the testing and isolation probability of infected individuals by around 5%, in order to get similar number of cumulative cases during the 60 days of meetings.

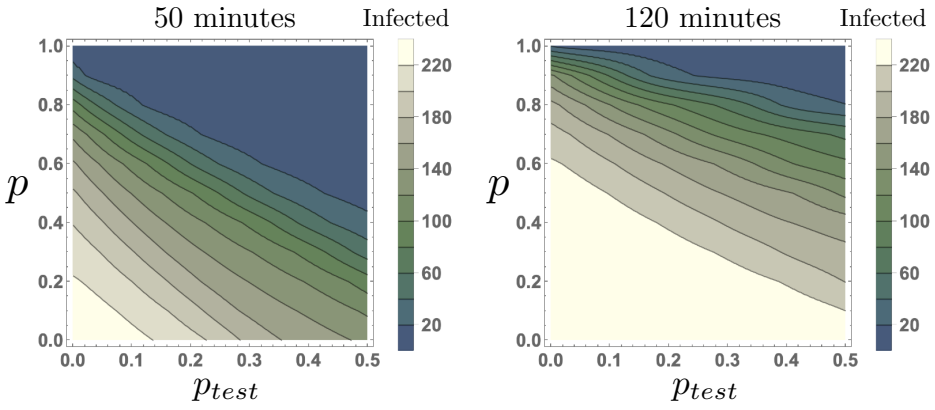

Fig. S15. Trade-off between testing (p_{test}), and mask compliance (d), on the cumulative number of secondary cases produced in 60 days having a single meeting, for the scenarios of meeting lengths of 50 and 120 minutes.

Figure S15 shows that the trade-off between testing/isolation and mask compliance follows a linear-like relationship. Moreover, our simulations show that that the trade-off between these control measures depends on the meeting length (T). For short meetings (50 minutes length), reducing 20% mask compliance would require to increase around 10% the probability of detecting and isolating infected individuals. In counterpart, for long meetings (120 minutes length), a reduction of 20% mask compliance would require to increase around 20% testing.

Finally, in this scenario we explore the trade-off between inter-meetings break times and testing.

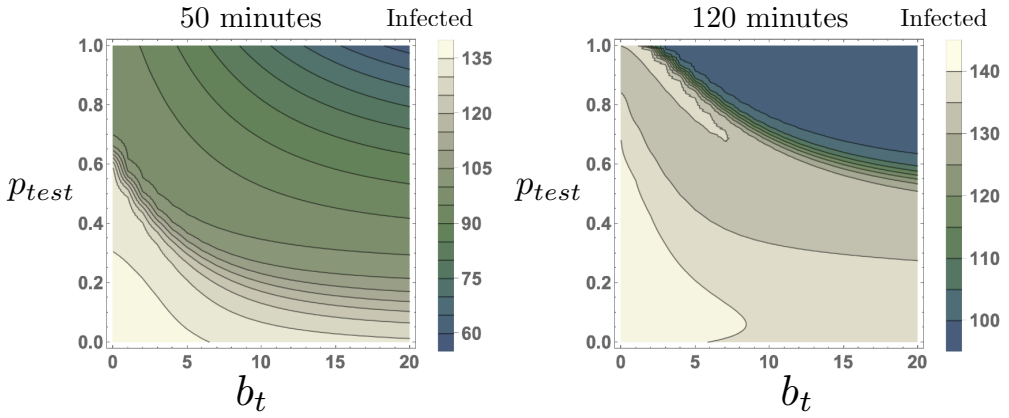

Fig. S16. The trade-off between testing (p_{test}) and break times (b_t) on the cumulative cases generated over 60 days assuming 6 daily meetings.

Figure S16 shows the non-linear trade-off between allowing break times between subsequent meetings, and the probability of detection/isolation of infected individuals. Notice that identifying and isolating all the infected individuals does not eradicate the epidemic. The reasoning behind this is that our model assumes only currently infected individuals are being tested, therefore newly infected individuals keep the viral load in the environment. Finally, our simulations suggest that, depending on the meeting length, there is a critical trade-off between testing and breaks time so that the number of cumulative cases dramatically increases. Particularly, for short meetings (50 minutes long), decreasing testing capacity by around 60% for a no breaks scenario, would be balanced by having breaks time of around 20 minutes. In counterpart, for long meetings (120 minutes long), the trade-off translates into a testing reduction of 40% of testing by increasing the break time to 20 minutes.

More complex epidemic models

In this section we show that the proposed framework can be coupled with more complex epidemic models. Specifically, we incorporate the role of exposed (pre-symptomatic individuals) and asymptomatic individuals in order to illustrate our modeling framework. The results of expanding the baseline SIR model to include exposed and asymptomatic health-states are consistent with literature as expected. Consequently, we do not expect our results to change qualitatively — we can expect our results would change quantitatively as different epidemic models are formulated.

Summary of observations. Although exposed individuals might exhibit a reduced viral shedding relative to symptomatic ones, incorporating infectious exposed individuals in our model (SEIR model), increases the viral load contribution of a typical infected individual by increasing its viral shedding time. This produces more secondary cases and increases the effort required to contain an outbreak. In contrast, the impact of assuming a fraction of the infected population become asymptomatic depends on both: (i) the relative infectiousness of asymptomatic individuals and, (ii) the fraction of asymptomatic cases. For COVID-19, it is possible to argue that asymptomatic individuals would exhibit an increased likelihood of infection, however we assume its viral shedding in the absence of symptoms is reduced, relative to symptomatic individuals. Finally, it is noteworthy that, while we consider discrete-time models in this work, similar formulation can be used to couple different modeling frameworks like continuous-time models and/or stochastic models.

SEIR model. Assume the within host disease progression is given by the following health-states: susceptible (S), exposed and infectious (E), infected and infectious (I), and fully immune recovered (R) individuals. We let the population to be composed of unmasked individuals $((1-p)G = S^n + E^n + I^n + R^n)$, and masked individuals $(pG = S^m + E^m + I^m + R^m)$. Susceptible individuals become infected by inhaling the

viral droplets exhaled by infectious exposed and symptomatic individuals. Infectious exposed individuals (E), are assumed to have a reduced viral shedding rate $\varepsilon\omega$, relative to infectious symptomatic individuals. Following the formulation of Eq. (4), the overall virus exhalation rate is given by

$$v = k\,(\underbrace{\eta I^m + I^n}_{\substack{\text{Viral shedding}\\ \text{symptomatic ind.}}} + \underbrace{\varepsilon(\eta E^m + E^n)}_{\substack{\text{Relative viral shedding}\\ \text{exposed ind.}}}),$$

where η stands for the reduced virus exhalation rate for masked individuals and, ε is the relative viral load of exposed individuals (E). Then, the infection probabilities' linear approximations become

$$P_n(T) = \omega\left(\eta I^m + I^n + \varepsilon(\eta E^m + E^n)\right) \quad \text{and} \quad P_m(T) = \alpha\omega\left(\eta I^m + I^n + \varepsilon(\eta E^m + E^n)\right),$$

where masked individuals are assumed to have a reduced virus exhalation of $\eta\omega$ and, a reduced virus inhalation $\alpha\omega$, where $0 \leq \eta, \alpha < 1$. Infectious exposed individuals (E), are assumed to have a reduced viral shedding rate $\varepsilon\omega$ relative to infectious symptomatic individuals and, to become symptomatic with probability σ. Symptomatic individuals (I) produce a baseline viral shedding, recovering with probability (ϕ). Finally, immune individuals are assumed to become fully susceptible with probability (λ). The previously described model of disease progression is shown schematically in Figure S17 and formalized by the sets of equations Eq. (38) and Eq. (39).

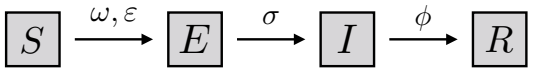

Fig. S17. Susceptible, infectious exposed (pre-symptomatic), infectious symptomatic and, recovered individuals. Infectious exposed individuals are assumed to have a reduced viral load relative to symptomatic individuals $0 \leq \varepsilon < 1$.

The disease progression among the unmasked population is described by the following set of equations, where the subscript tracks the evolution of states in time, while the superscript tracks the population mask usage

$$\begin{aligned}
(1-p)G &= S_j^n + E_j^n + I_j^n + R_j^n,\\
S_{j+1}^n &= \left(1 - \omega\left(\eta\, I_j^m + I_j^n + \varepsilon(\eta E_j^m + E_j^n)\right)\right) S_j^n + \underbrace{\lambda}_{\substack{\text{Waning immunity}\\ \text{probability}}} R_j^n,\\
E_{j+1}^n &= \underbrace{\omega\left(\eta\, I_j^m + I_j^n + \varepsilon(\eta E_j^m + E_j^n)\right)}_{\substack{\text{Infection}\\ \text{probability}}} S_j^n + (1-\sigma) E_j^n,\\
I_{j+1}^n &= \underbrace{\sigma}_{\substack{\text{Probability of}\\ \text{developing symptoms}}} E_j^n + (1-\phi) I_j^n,\\
R_{j+1}^n &= \underbrace{\phi}_{\substack{\text{Recovery}\\ \text{probability}}} I_j^n + (1-\lambda_P) R_j^n;
\end{aligned} \tag{38}$$

similarly, the progression of the disease among the masked population is described by the following equations,

where the mask reduces the virus inhalation, re-scaling the infection probability by a factor α

$$
\begin{aligned}
pG &= S_j^m + E_j^m + I_j^m + R_j^m, \\
S_{j+1}^m &= \Big(1 - \alpha\omega\left(\eta\, I_j^m + I_j^n + \varepsilon(\eta E_j^m + E_j^n)\right)\Big) S_j^m + \lambda R_j^m, \\
E_{j+1}^n &= \alpha\,\omega\left(\eta\, I_j^m + I_j^n + \varepsilon(\eta E_j^m + E_j^n)\right) S_j^m + (1-\sigma) E_j^m, \\
I_{j+1}^m &= \sigma E_j^m + (1-\phi) I_j^m. \\
R_{j+1}^m &= \phi_P I_j^m + (1-\lambda_P) R_j^m.
\end{aligned}
\qquad [39]
$$

Steady state when all or none wear masks. Assume the extreme scenario where nobody uses masks. We compute the steady state by solving the system of equations $\{S_j = S^*, E_j = E^*, I_j = I^*, R_j = R^*\}$. The non-trivial steady state of model Eq. (38) is given by

$$
\{S^*, E^*, I^*, R^*\} = \left\{ \frac{\sigma\phi}{\omega(\sigma+\varepsilon\phi)}, \frac{\lambda\phi}{\varphi}\left(G - \frac{\sigma\phi}{\omega(\sigma+\varepsilon\phi)}\right), \frac{\lambda\sigma}{\varphi}\left(G - \frac{\sigma\phi}{\omega(\sigma+\varepsilon\phi)}\right), \frac{\sigma\phi}{\varphi}\left(G - \frac{\sigma\phi}{\omega(\sigma+\varepsilon\phi)}\right) \right\}. \qquad [40]
$$

where $\varphi = \sigma\phi + \lambda(\sigma+\phi)$. Furthermore, we compute the basic reproductive number by using the second generation matrix method, $\mathcal{R}_0 = G\omega\left(\frac{1}{\phi} + \frac{\varepsilon}{\sigma}\right)$. Therefore, the impact of the exposed (pre-symptomatic) and asymptomatic individuals on the within-meeting viral load depends on their relative viral shedding ($\varepsilon_E\omega$ and $\varepsilon_A\omega$), and their relative incubation period ($1/\sigma$). The steady state of the scenario where everybody uses masks is similar, including the mask efficiency factors α and η.

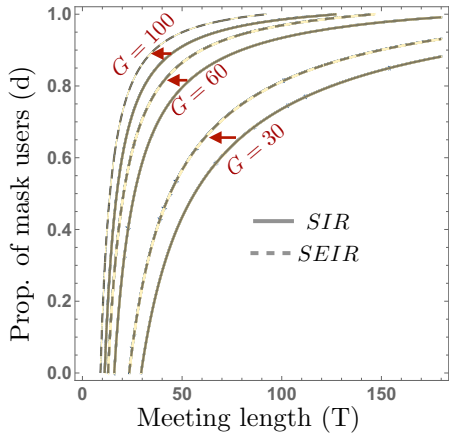

Fig. S18. Disease eradication threshold as a function of the meeting length and the proportion of the population wearing masks, for the SIR and SEIR disease models.

Figure S18 shows the comparison of the effort needed in order to eradicate an outbreak for the SIR and SEIR models. We assume exposed (pre-symptomatic) individuals are 50% less infectious than symptomatic individuals, and an incubation period of 9 days. Notice that the presence of infectious pre-symptomatic individuals increases the effort needed in order to eradicate an outbreak, relative to the scenario of having no pre-symptomatic individuals.

SEIAR model. Assume the within host disease progression is given by the following health-states: susceptible (S), exposed and infectious (E), infected and infectious (I), infectious asymptomatic (A), and fully immune recovered (R) individuals. Similar to the previous model we assume the total population is composed by unmasked and masked individuals, $(1-p)G$ and pG, respectively. Susceptible individuals get infected by inhaling droplets exhaled by: (i) infectious exposed individuals (E) at a relative shedding

rate $\varepsilon_E\omega$, (ii) asymptomatic infectious individuals at a relative shedding rate $\varepsilon_A\omega$ and, (iii) infectious individuals at a baseline rate. Similar to the previous section, we let the virus exhalation rate to become

$$v = k\,(\underbrace{\eta I^m + I^n}_{\substack{\text{Viral shedding}\\ \text{symptomatic ind.}}} + \underbrace{\varepsilon(\eta E^m + E^n)}_{\substack{\text{Relative viral shedding}\\ \text{exposed ind.}}} + \underbrace{\varepsilon_A(\eta A^m + A^n)}_{\substack{\text{Relative viral shedding}\\ \text{asymptomatic ind.}}}),$$

then the infection probabilities linear approximations become

$$\begin{aligned} P_n(T) &= \omega\left(\eta I^m + I^n + \varepsilon_E(\eta E^m + E^n) + \varepsilon_A(\eta A^m + A^n)\right),\\ P_m(T) &= \alpha\omega\left(\eta I^m + I^n + \varepsilon_E(\eta E^m + E^n) + \varepsilon_A(\eta A^m + A^n)\right), \end{aligned} \qquad [41]$$

where ε_E and ε_A are the reduced viral shedding of exposed (E) and asymptomatic individuals (A) respectively, relative to symptomatic individuals (I). The previously formulated model of disease progression is sketched in Figure S19 and formalized by the set of equations Eq. (42).

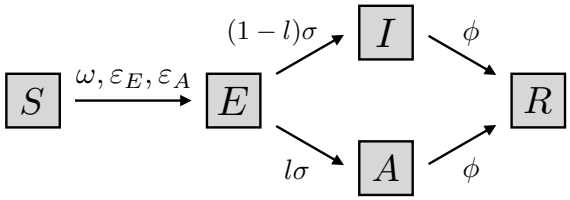

Fig. S19. Susceptible, infectious exposed (pre-symptomatic), infectious symptomatic, infectious asymptomatic and, recovered individuals. Infectious exposed and asymptomatic individuals are assumed to have reduced viral shedding relative to symptomatic individuals, $0 \leq \varepsilon_E, \varepsilon_A < 1$, respectively.

$$\begin{aligned} (1-p)G &= S_j^n + E_j^n + I_j^n + A_j^n + R_j^n,\\ S_{j+1}^n &= \left(1 - \omega\left(\eta\, I_j^m + I_j^n + \varepsilon_E(\eta E_j^m + E_j^n) + \varepsilon_A(\eta A^m + A^n)\right)\right)S_j^n + \lambda R_j^n\\ E_{j+1}^n &= \omega\left(\eta\, I_j^m + I_j^n + \varepsilon_E(\eta E_j^m + E_j^n) + \varepsilon_A(\eta A^m + A^n)\right)S_j^n + (1-\sigma)E_j^n,\\ I_{j+1}^n &= (1-l)\sigma E_j^n + (1-\phi)I_j^n,\\ A_{j+1}^n &= l\sigma E_j^n + (1-\phi)A_j^n,\\ R_{j+1}^n &= \phi(I_j^n + A_j^n) + (1-\lambda_P)R_j^n,\\ pG &= S_j^m + E_j^m + I_j^m + A_j^m + R_j^m,\\ S_{j+1}^m &= \left(1 - \alpha\omega\left(\eta\, I_j^m + I_j^n + \varepsilon_E(\eta E_j^m + E_j^n) + \varepsilon_A(\eta A^m + A^n)\right)\right)S_j^m + \lambda R_j^m\\ E_{j+1}^m &= \alpha\omega\left(\eta\, I_j^m + I_j^n + \varepsilon_E(\eta E_j^m + E_j^n) + \varepsilon_A(\eta A^m + A^n)\right)S_j^m + (1-\sigma)E_j^m,\\ I_{j+1}^m &= (1-l)\sigma E_j^m + (1-\phi)I_j^m,\\ A_{j+1}^m &= l\sigma E_j^m + (1-\phi)A_j^m,\\ R_{j+1}^m &= \phi(I_j^m + A_j^m) + (1-\lambda)R_j^m. \end{aligned} \qquad [42]$$

A. Basic reproductive number when all or none wear masks. Assume nobody wear masks, in this scenario the basic reproductive number becomes $\mathcal{R}_0 = G\omega\left(\frac{\varepsilon_E}{\sigma} + \frac{(1-l)+l\varepsilon_A}{\phi}\right)$. The first term of $\mathcal{R}_0$ accounts

for contributions from the mildly infectious individuals E, whereas the second term gives contributions from the infectious individuals I and, the mildly infectious individuals A.

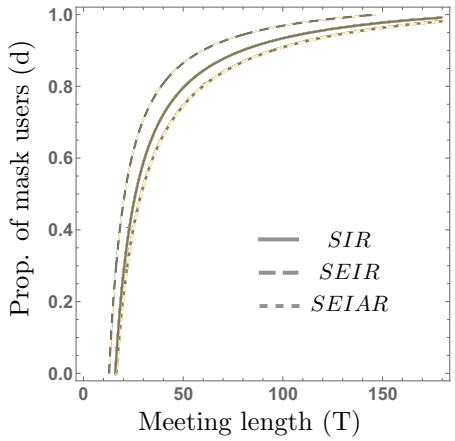

Fig. S20. Disease eradication threshold as a function of the meeting length and the proportion of the population wearing masks; for the SIR, SEIR and SEIAR disease models and, $G = 60$.

Figure S20 shows the disease eradication threshold for a group size of $G = 60$, as a function of both, the meeting length (T) and the proportion of the population wearing masks (d). The impact of asymptomatic individuals with a reduced viral shedding (relative to the symptomatic individuals) is reflected on the relaxed effort required to eradicate an outbreak.

SEIAR model with recruitment. Assume the within host disease progression is given by susceptible (S), exposed and infectious (E), infected and infectious (I), infectious asymptomatic (A), and fully immune recovered (R) individuals. Moreover, assume individuals might decide to leave at a given time with probability μ regardless of their health-status. Additionally, assume non-symptomatic individuals (S, E, R), are allowed to join to the group at a constant probability Λ. This might be for instance monitored by testing before joining. In this scenario, and following similar assumptions than for the previous SEIAR model, the model of disease progression among the masked/unmasked population is depicted in Figure and, formalized by the set of difference equations Eq. (43) and Eq. (44)

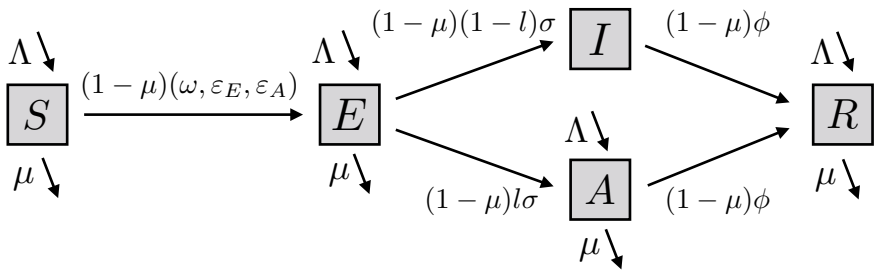

Fig. S21. Susceptible, infectious exposed (pre-symptomatic), infectious symptomatic, infectious asymptomatic and, recovered individuals. Infectious exposed and asymptomatic individuals are assumed to have reduced viral shedding relative to symptomatic individuals, $0 \leq \varepsilon_E, \varepsilon_A < 1$, respectively. Moreover, constant recruitment into non-symptomatic health-states and, leaving rate regardless individuals' health states are assumed.

$$
\begin{aligned}
(1-p)G &= S_j^n + E_j^n + I_j^n + A_j^n + R_j^n, \\
S_{j+1}^n &= \underbrace{\Lambda}_{\substack{\text{Individuals}\\ \text{joining}}} + \underbrace{(1-\mu)}_{\substack{\text{Probability of}\\ \text{keep meeting}}} \Big(1 - \omega\left(\eta\, I_j^m + I_j^n + \varepsilon_E(\eta E_j^m + E_j^n) + \varepsilon_A(\eta A^m + A^n)\right)\Big) S_j^n \\
&\quad + \underbrace{\lambda}_{\substack{\text{Waning immunity}\\ \text{probability}}} R_j^n, \\
E_{j+1}^n &= \Lambda + (1-\mu)\underbrace{\omega\left(\eta\, I_j^m + I_j^n + \varepsilon_E(\eta E_j^m + E_j^n) + \varepsilon_A(\eta A^m + A^n)\right)}_{\substack{\text{Infection}\\ \text{probability}}} S_j^n + (1-\mu)(1-\sigma)E_j^n, \\
I_{j+1}^n &= (1-\mu)\underbrace{(1-l)\sigma}_{\substack{\text{Probability of}\\ \text{developing symptoms}}} E_j^n + (1-\mu)(1-\phi)I_j^n, \\
A_{j+1}^n &= \Lambda + (1-\mu)\underbrace{l\sigma}_{\substack{\text{Probability of}\\ \text{becoming asymptomatic}}} E_j^n + (1-\mu)(1-\phi)A_j^n, \\
R_{j+1}^n &= \Lambda + (1-\mu)\underbrace{\phi}_{\substack{\text{Recovery}\\ \text{probability}}} (I_j^n + A_j^n) + (1-\mu)(1-\lambda_P)R_j^n.
\end{aligned}
$$

[43]

Similarly, the progression of the disease among the masked population is described by the following analogous equations, where the mask reduces the virus inhalation, re-scaling the infection probability by a factor α

$$
\begin{aligned}
pG &= S_j^m + E_j^m + I_j^m + A_j^m + R_j^m, \\
S_{j+1}^m &= \Lambda + (1-\mu)\Big(1 - \alpha\omega\left(\eta\, I_j^m + I_j^n + \varepsilon_E(\eta E_j^m + E_j^n) + \varepsilon_A(\eta A^m + A^n)\right)\Big) S_j^m + \lambda R_j^m, \\
E_{j+1}^m &= \Lambda + (1-\mu)\alpha\omega\left(\eta\, I_j^m + I_j^n + \varepsilon_E(\eta E_j^m + E_j^n) + \varepsilon_A(\eta A^m + A^n)\right) S_j^m + (1-\mu)(1-\sigma)E_j^m, \\
I_{j+1}^m &= (1-\mu)(1-l)\sigma E_j^m + (1-\mu)(1-\phi)I_j^m, \\
A_{j+1}^m &= \Lambda + (1-\mu)l\sigma E_j^m + (1-\mu)(1-\phi)A_j^m, \\
R_{j+1}^m &= \Lambda + (1-\mu)\phi(I_j^m + A_j^m) + (1-\mu)(1-\lambda)R_j^m.
\end{aligned}
$$

[44]

In this formulation, the total group size is not constant and, the total group size follows the difference equation

$$G_{j+1} = 8\Lambda + (1-\mu)G_j \qquad [45]$$

which implies an asymptotically constant total group size (19). By solving Eq. (45), the group size is given by $\lim_{j\to\infty} G_j = \frac{8\Lambda}{\mu}$.

Case studies

In this section we illustrate the value of our framework in addressing different room types. Following (13), we study three scenarios of contagion: (i) a typical American classroom, with an occupancy of 20 individuals

and a volume of $V = 10595\ ft^3$, meeting during 6 hours; (ii) long-term care facilities, which in New York City are required to host a maximum of 3 persons in a shared room with a volume of $V = 1890\ ft^3$; and, (iii) the Skagit valley choir super-spreading event, which is reported to have happened in a room hosting 61 during a 2.5 hrs. We assume the individuals meeting exhibit different virus shedding rates, where the baseline virus shedding rate $(k = 1)$, correspond to individuals breathing at rest. Individuals speaking show an increment of the shedding rate or infection quanta of 300% at the intermediate activity level, while at the high activity level there is an increment of 800% for intermediate speech.

Classroom. We assume the scenario of a classroom with occupancy of 19 students and a teacher, meeting during a week. For our baseline simulations we assumed 50% of the group use masks ($p = 0.5$), but we explore the impact of varying both, mask usage and the break time. We assume the break time corresponds to recess during which the room is empty and cleaning through a ventilation system during 30 minutes. Our selected simulations show the disease dynamics within a classroom for low activity level (breathing at rest), medium activity level (quiet speech) and, high activity (intermediate speech); these correspond to 8.8, 29 and 72 infection $quanta\ /m^3$ exhaled air (13).

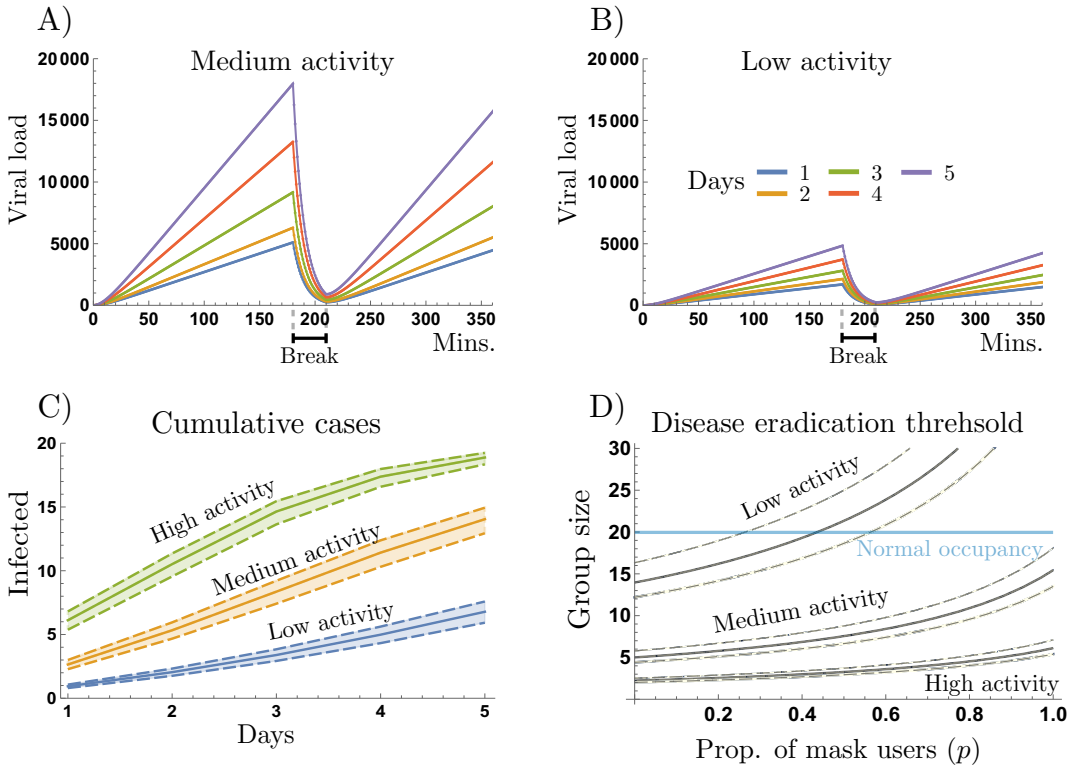

Fig. S22. Disease dynamics within a typical US classroom during a week, for low, medium and, high activity levels. Panel A and panel B show the viral load attained during a school day for five days, for the scenarios where individuals sustain high and low activity, respectively. Panel C shows the cumulative secondary cases generated within the classroom over the 5 days; while panel D shows the proportion of mask users and the group size trade-off required to prevent a single infection within the classroom, for the scenarios of low, medium and high activity levels. We assumed uncertainty boundaries corresponding to $\pm 15\%$ of the baseline breathing activity.

High activity breathing levels within a classroom elevate the viral load in a dramatic way compared to the viral low attained with low breathing levels, as our simulations in panels A and B show. This impact on the expected secondary cases generated at a single day and, ultimately impacts the progression of the epidemic (panel C). Panel D shows the disease eradication threshold as a function of both, the proportion of mask users (p) and, the group size (G), for activity levels corresponding to breathing at rest, quiet speech and intermediate speech. We assume students meet during 5 consecutive days and leave the classroom during a

recess of 30 mins. after 3 hours of meeting. Our results highlight the trade-off between a decentralized control measure (maks-wearing) and, a centralized control measure (group size and breaks time).

Long-term care facility. In this section we assume the scenario of infections among individuals in a long-term care facility. In order to address the higher susceptibility of elderly people we let them to be four times more susceptible than child (20, 21). Figure S23A shows the expected cumulative cases among three persons sharing a room $24\,hrs/day$ during 5 days, where all of them wear face masks. For medium and high activity levels our simulations suggest that masking and the baseline air filtering are not enough to avoid infections. Figure S23B shows the disease eradication threshold as a function of the proportion of mask users (p) and, the group size (G). Our simulations show that for low and medium breathing levels, for normal occupancy, on average at least two residents should use mask in order to prevent infections during a days period.

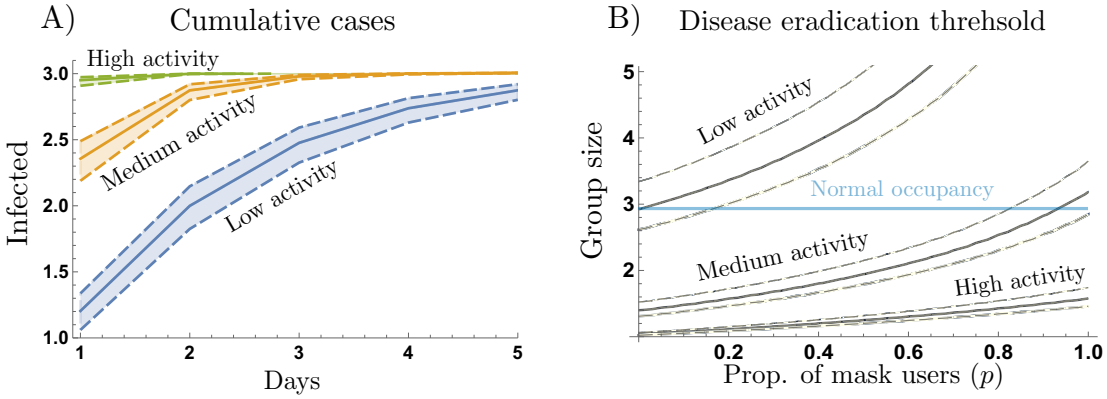

Fig. S23. Disease dynamics among three elderly people sharing room in a long-term care facility. Panel A shows that even when all are masked, it is expected to have infections for low activity level of breathing at rest. Panel B shows the disease threshold conditions to avoid infections as a function of the proportion of mask users (p) and, the group size sharing a room, for activity levels of low, medium and high activity levels. We assumed uncertainty boundaries corresponding to $\pm 15\%$ of the baseline breathing activity.

The Skagit Valley Choir. Here we study the contagion process of the superspreading event during the Skagit Valley Choir practice on March 10, 2020 (5, 22). The practice lasted 2.5 hrs and, 61 persons attended the choir practice, after which 32 COVID-19 cases were confirmed and 20 more resulted probable secondary cases. It is known that this event started with a single confirmed symptomatic individual and, transmission was potentially exacerbated by the close proximity among attendants (within 6 feet) and, by the high breathing level by the act of singing (22). Previous studies indicate that an estimation of the emission rate is $970 \pm 390\,quanta/h$ (5), which in our framework it translates to $k = 110$, given that the baseline $k = 1$ value corresponds to nose-nose breathing activity of $8.8\,quanta\,/m^3$ exhaled air. We assume none of the choir members used face masks $p = 0$, a single symptomatic case $I_0 = 1$ and $E_0 = 10$ pre-symptomatic individuals potentially infected before the practice on March 10, for a detailed discussion see (5, 22).

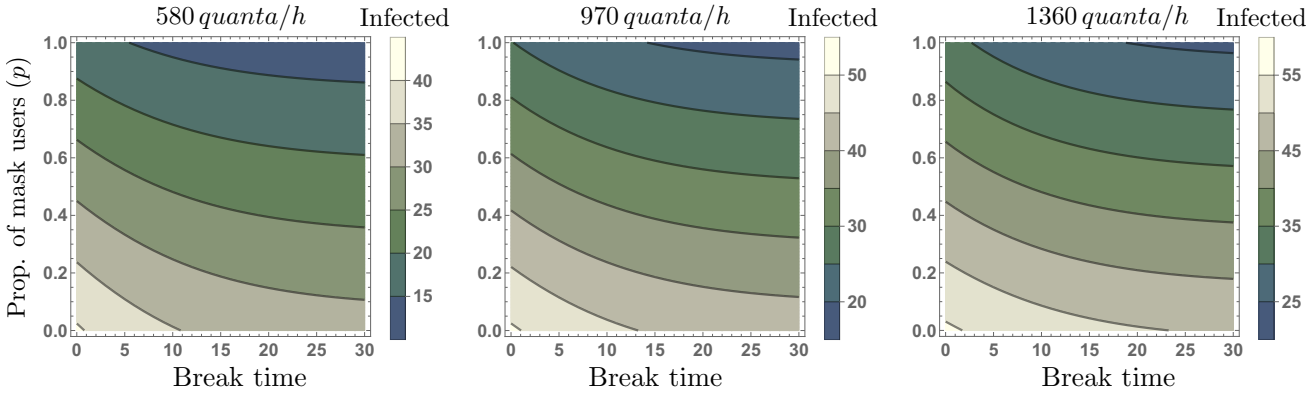

Fig. S24. Number of infected after the members of the Skagit Valley Choir have a single meeting for 2.5 hrs, as a function of the break time and the proportion of masked individuals. We consider the baseline emission rate ($970\ quanta/h$) and the uncertainty boundaries ($970 \pm 390\ quanta/h$.)

Our simulations in Figure S24 shows the potential reduction on the number of secondary infections produced during the 2.5 hr. choir meeting, as a function of the break time and the proportion of masked individuals. In the absence of masks, a single break of would have reduced the number of infections significantly. Moreover, combining a single break time and at least 40% of mask compliance would have reduced the number of infections by around half.

Summary. Our results highlight the impact of the multiple components involved in our modeling framework: breathing activity, group size, meeting schedule, inter-meetings breaks and, mask compliance. Increasing mask compliance relax the required conditions to avoid the disease to spread; however, the activity level shows to be highly determinant in each of the scenarios. On the other hand, under compliance uncertainty of decentralized control measures (for instance, mask wearing or social distancing), the incorporation of centralized measures (for instance, break times, isolation or testing), is critical to avoid high viral load levels.

Table S4. Results case studies

Case study	Room size ($ft.^3$)	Group size	Meetings schedule	Findings
Classroom	10595	20	2 meetings / 5 days	Break times play a critical role Small group sizes also require high mask compliance.
Long-term care facility	1890	3	1 meeting / 5 days	The high vulnerability of elderly people requires high masking levels if breathing activity is medium or high.
Skagit valley choir	28605	61	1 meeting	A single break time combined with medium mask compliance would have reduced by half the infections.

i

References

1. WF Wells, , et al., Airborne contagion and air hygiene. an ecological study of droplet infections. *Airborne Contagion Air Hyg. An Ecol. Study Droplet Infect.* (1955).
2. RL Riley, Airborne infection. *The Am. journal medicine* **57**, 466–475 (1974).
3. E Riley, G Murphy, R Riley, Airborne spread of measles in a suburban elementary school. *Am. journal epidemiology* **107**, 421–432 (1978).
4. L Gammaitoni, MC Nucci, Using a mathematical model to evaluate the efficacy of tb control measures. *Emerg. infectious diseases* **3**, 335 (1997).
5. SL Miller, et al., Transmission of sars-cov-2 by inhalation of respiratory aerosol in the skagit valley chorale superspreading event. *Indoor air* **31**, 314–323 (2021).

6. PS Dodds, DJ Watts, A generalized model of social and biological contagion. *J. theoretical biology* **232**, 587–604 (2005).
7. H Jang, et al., Evaluating architectural changes to alter pathogen dynamics in a dialysis unit in *2019 IEEE/ACM International Conference on Advances in Social Networks Analysis and Mining (ASONAM)*. (IEEE), pp. 961–968 (2019).
8. A Hekmati, M Luhar, B Krishnamachari, M Matarić, Simulating covid-19 classroom transmission on a university campus. *Proc. Natl. Acad. Sci*. **119**, e2116165119 (2022).
9. G Buonanno, L Stabile, L Morawska, Estimation of airborne viral emission: Quanta emission rate of sars-cov-2 for infection risk assessment. *Environ. international* **141**, 105794 (2020).
10. R Zafarnejad, PM Griffin, Assessing school-based policy actions for covid-19: An agent-based analysis of incremental infection risk. *Comput. Biol. Medicine* **134**, 104518 (2021).
11. N Loy, A Tosin, A viral load-based model for epidemic spread on spatial networks. *arXiv preprint arXiv:2104.12107* (2021).
12. PI Frazier, et al., Modeling for covid-19 college reopening decisions: Cornell, a case study. *Proc. Natl. Acad. Sci*. **119**, e2112532119 (2022).
13. MZ Bazant, JW Bush, A guideline to limit indoor airborne transmission of covid-19. *Proc. Natl. Acad. Sci*. **118**, e2018995118 (2021).
14. C Noakes, C Beggs, P Sleigh, K Kerr, Modelling the transmission of airborne infections in enclosed spaces. *Epidemiol. & Infect*. **134**, 1082–1091 (2006).
15. CM Issarow, N Mulder, R Wood, Modelling the risk of airborne infectious disease using exhaled air. *J. theoretical biology* **372**, 100–106 (2015).
16. A Foster, M Kinzel, Estimating covid-19 exposure in a classroom setting: A comparison between mathematical and numerical models. *Phys. Fluids* **33**, 021904 (2021).
17. LD Knibbs, L Morawska, SC Bell, The risk of airborne influenza transmission in passenger cars. *Epidemiol. & Infect*. **140**, 474–478 (2012).
18. X Gao, Y Li, GM Leung, Ventilation control of indoor transmission of airborne diseases in an urban community. *Indoor Built Environ*. **18**, 205–218 (2009).
19. P Van den Driessche, AA Yakubu, Disease extinction versus persistence in discrete-time epidemic models. *Bull. mathematical biology* **81**, 4412–4446 (2019).
20. NG Davies, et al., Age-dependent effects in the transmission and control of covid-19 epidemics. *Nat. medicine* **26**, 1205–1211 (2020).
21. S Garg, et al., Hospitalization rates and characteristics of patients hospitalized with laboratory-confirmed coronavirus disease 2019—covid-net, 14 states, march 1–30, 2020. *Morb. mortality weekly report* **69**, 458 (2020).
22. L Hamner, High sars-cov-2 attack rate following exposure at a choir practice—skagit county, washington, march 2020. *MMWR. Morb. mortality weekly report* **69** (2020).